Massive Stars as Tracers for Stellar & Galactochemical Evolution

Norbert Przybilla

Massive Stars as Tracers for Stellar & Galactochemical Evolution

Habilitationsschrift

der Naturwissenschaftlichen Fakultät

der

Friedrich-Alexander Universität Erlangen-Nürnberg

vorgelegt von

Norbert Przybilla

aus Kosel

Bamberg, den 25. September 2008

Fachmentorat:

Prof. Dr. E. Steffens (Vorsitzender)

Prof. Dr. U. Heber

Prof. Dr. W.-R. Hamann (Universität Potsdam)

It is also a good rule not to put overmuch confidence in the observational results that are put forward until they are confirmed by theory.

– SIR ARTHUR STANLEY EDDINGTON

Zusammenfassung

Heiße, massereiche Sterne nehmen eine Schlüsselstellung im Universum ein, als treibende Kraft des kosmischen Materiekreislaufes. Die Energie- und Impulsbilanz des interstellaren Mediums wird durch die ionisierende Strahlung massereicher Sterne, durch ihre Sternwinde und Supernova-Explosionen dominiert. Massereiche Sterne sind ebenfalls wichtige Stätten der Nukleosynthese. Aufgrund ihrer hohen absoluten visuellen Helligkeit eignen sie sich besonders gut für bodengebundene spektroskopische Beobachtungen. Mit Hilfe der heutigen Generation von Teleskopen der 8–10m-Klasse und modernen Instrumenten können massereiche Sterne in der Milchstraße, anderen aktiv sternbildenden Galaxien der Lokalen Gruppe, und sogar in Sternsystemen jenseits der Lokalen Gruppe spektroskopiert werden. Dies gestattet eine Bestimmung der chemischen Zusammensetzung der kosmischen Materie bis in große Distanzen. Die häufigsten massereichen Sterne, OB-Sterne im Massenbereich von etwa 8 bis $30\,M_{\odot}$, sind von besonderem Interesse für unsere Arbeit. Sie werden von uns auf homogene Weise von der Hauptreihe bis in späte Entwicklungsstadien als Überriesen der Spektraltypen B und A untersucht.

Quantitative Analysen von Sternen frühen Spektraltyps waren in der Vergangenheit nicht genau genug um wirklich aussagekräftig zu sein – so konnten Elementhäufigkeiten höchstens auf einen Faktor $\sim$2 genau bestimmt werden. Wir haben daher entscheidende Verbesserung an den Modellen und der Analysemethodik vorgenommen. Eine zentrale Rolle spielen dabei Modellatome, für deren Erstellung die präzisesten zur Verfügung stehenden Atomdaten verwendet wurden, und die Identifikation und konsequenten Reduktion/Eliminierung von Quellen systematischer Fehler. Sternparameter und Elementhäufigkeiten lassen sich dadurch mit weit höherer Genauigkeit bestimmen als jemals zuvor. Die Früchte unserer Bemühungen stellen sich wie folgt dar: Unsicherheiten in der Bestimmung stellarer Effektivtemperaturen konnten auf weniger als $\sim$1–2% gedrückt werden, auf $\sim$10–25% für die Schwerebeschleunigung an der Sternoberfläche und auf $\sim$10–25% (statistischer) und $\sim$15–25% (systematischer 1σ-Fehler) für Elementhäufigkeiten. Massereiche Sterne werden dadurch zu universellen Werkzeugen für die Präzisionsdiagnostik in der moderne Astrophysik.

Wir haben unsere neue Analysetechnik auf hochaufgelöste Spektren von B-Hauptreihen-Sternen und BA-Überriesen in der Milchstraße und anderen Galaxien angewendet. Die Analyseergebnisse sind wichtig für das Verständnis der Entwicklung massereicher Sterne und der chemischen Entwicklung von Galaxien, insbesondere der Milchstraße, da erstmalig fundierte Schlüsse gezogen werden können. Die Häufigkeiten der leichten Elemente (He, C, N) liefern Hinweise darauf, wie komplexe (magneto-)hydrodynamische Prozesse im Sterninnern die Sternentwicklung beeinflussen. Anhand der Häufigkeiten der schweren Elemente lässt sich die Metallizitätsverteilung innerhalb einer Galaxis kartieren. Zu unseren wichtigsten Resultaten zählen: I) die Effizienz von Mischprozessen im Sterninnern ist um etwa einen Faktor 2 höher als von etablierten Sternentwicklungsmodellen für rotierende Sterne vorhergesagt. II) Junge massereiche Sterne der Sonnenumgebung weisen entgegen gängiger Lehrmeinung eine sehr ähnliche chemische Zusammensetzung auf. III) Die daraus ermittelten Referenzwerte

für Elementhäufigkeiten (den "kosmischen Häufigkeitsstandard", in Anlehnung an den solaren Standard) nutzen wir, um auf die chemischen Zusammensetzung des interstellaren Staubs rückzuschließen. IV) Die galaktische Scheibe weist entgegen gängiger Vorstellungen einen flachen Häufigkeitsgradienten auf, bei insgesamt hohem Metallgehalt und geringer Streuung. V) Erste Resultate von Untersuchungen massereicher Überriesen in anderen Galaxien der Lokalen Gruppe und darüber hinaus werden diskutiert. Dabei wird Pionierarbeit auf dem jungen Gebiet der Extragalaktischen Stellarastronomie geleistet. VI) Schließlich wenden wir unsere Analysetechnik auf hochaufgelöste Spektren von drei Objekten einer neuentdeckten Sternklasse an – Flüchtlinge der Milchstraße, so genannte "Hyper-Velocity Sterne" (HVS). Dabei erweist sich HVS 7 als ein chemisch sehr pekuliärer Hauptreihenstern. HVS 3 entstammt – entgegen der Erwartung – nicht der Milchstraße; seine chemische Zusammensetzung entspricht der von Sternen der Großen Magellanschen Wolke, womit ein Ursprung in unserer Nachbargalaxie nachgewiesen ist. HD 271791 wird als Überlebender einer Supernovaexplosion in einem Doppelsternsystem identifiziert. Der Stern stellt den ersten Vertreter einer neuen Kategorie von "Hyper-Runaway Sternen" dar.

Contents

Abstract

Hot, massive stars are key drivers of the cosmic cycle of matter. They are the dominant contributors to the energy and momentum budget of the interstellar medium, via ionizing radiation, stellar winds and supernova explosions, and they are important sites of nucleosynthesis. Because of their high luminosities these stars are primary targets for spectroscopy over large distances. With the present generation of 8-10m-class telescopes and modern instruments they can be used as powerful tracers of chemical composition throughout the Milky Way, other star-forming galaxies of the Local Group, and even in systems beyond the Local Group. The most frequent massive stars, OB-type stars in the mass range from about 8 to 30 $M_{\odot}$, are of particular interest to us, which are studied in a homogeneous way from the main sequence to the evolved stage as BA-type supergiants.

In the past, quantitative studies of early-type stars were not accurate enough – e.g. only to within a factor $\sim$2 at most for elemental abundances – to derive conclusive results. Here we summarise our advances made in the modelling and the analysis methodology. Now, quantitative spectroscopy allows stellar parameters and chemical abundances of these objects to be constrained with much higher precision than previously possible: to $\lesssim$1–2% uncertainty in effective temperature, $\sim$10–25% in surface gravity, and $\sim$10–25% (random) plus $\sim$15–25% (systematic 1σ-errors) in elemental abundances. This is achieved by the use of improved atomic data and the identification and consequent reduction of systematic errors. Massive stars are thus turned into universal tools for modern astrophysics.

The improved model atmosphere analyses have a strong impact on our understanding of the evolution of massive stars and the chemical evolution of galaxies, as thorough conclusions can be drawn for the first time. We discuss massive stars as tracers for: I) abundances of the light elements, which make possible the study of the effects of complex (magneto-)hydrodynamic mixing processes in the stellar interior that govern stellar evolution; II) the abundances of the heavier elements, which allow the present-day spatial distribution of metals in the Milky Way and other galaxies to be investigated. The most prominent results are: I) mixing efficiencies are higher than predicted by standard evolution models for rotating massive stars, by about a factor 2; II) the young stellar component in the solar neighbourhood is chemically homogeneous, the resulting cosmic abundance standard facilitating tight constraints to be put on the dust-phase composition of the interstellar medium for the first time; III) a flat abundance gradient is found for the Galactic disk, indicating overall high metallicity and little abundance scatter. Finally, first results from studies of massive supergiants in other galaxies within the Local Group and beyond are discussed, pioneering the new field of extragalactic stellar astronomy. Attention is drawn in particular to galactic abundance gradients and a novel spectroscopic distance determination technique. The gap between Galactic and extragalactic research is bridged by a newly discovered class of stars – objects unbound to the Galaxy –, the so-called hyper-velocity stars (HVSs). First quantitative studies find the survivor of a binary supernova, an unexpected origin of a second HVS in the Large Magellanic Cloud, and identify a third HVS as an unusual chemically peculiar magnetic star.

1 Introduction

Cosmology, the formation and evolution of galaxies, and the cosmic cycle of matter pose major challenges for modern astronomy. Stars have been the driving force of evolution ever since the Cosmic Dark Ages. Massive stars are of particular importance as sites of nucleosynthesis and as dominant contributors to the energy and momentum budget of the interstellar medium (ISM), via ionizing radiation, stellar winds and supernova explosions (SNe).

One cornerstone in the wide field of galaxy evolution is the investigation of the chemical evolution of the Milky Way (e.g. Pagel 1997; Matteucci 2001). Here, the predictive power of different model scenarios (among the more recent work e.g. Hou et al. 2000; Chiappini et al. 2001, 2003; Oey 2003; Kobayashi et al. 2006; Cescutti et al. 2007) can be verified in great detail by comparison with observation. The solar neighbourhood[1] is of particular interest. Long-lived low-mass stars in the solar neighbourhood play an important rôle, as they allow the evolution of the Galaxy to be studied over time (e.g. Edvardsson et al. 1993; Fuhrmann 1998, 2008, and references therein; Gratton et al. 2003; Bensby et al. 2003; Cayrel et al. 2004; Honda et al. 2004). In order to sample larger distances, more luminous indicators are required, like H II regions or massive stars. These short-lived objects trace present-day abundances only. However, they provide important information complementary to low-mass cool stars: they allow elemental abundances to be sampled spatially over the entire disk of the Milky Way.

The drivers behind the evolution of the Galaxy are the stars. Massive ones determine the pace because of their short life cycles. Only the massive stars pass through all (static) fusion cycles up to silicon burning, preparing the seed for the synthesis of the heaviest elements (Burbidge et al. 1957; Cameron 1957) in SNe type II. A quantitative understanding of the evolution of massive stars is therefore essential for the deeper study of the whole picture.

Models of massive star evolution have attained a high degree of sophistication recently. Models accounting for effects of mass-loss and rotation (Heger & Langer 2000; Maeder & Meynet 2000) succeeded in reproducing observed abundance patterns in massive stars. In particular, enriched helium and nitrogen, and depleted carbon are indicative for the mixing of nuclear-processed matter from the stellar core to the atmosphere, which can be observed in fast-rotating stars even on the main sequence. More recent developments concentrated on the interplay of rotation and magnetic fields (Heger et al. 2005; Maeder & Meynet 2005), which – depending on the input physics – may result in quantitatively different predictions for the amount of chemical mixing. Systematic investigations of massive stars of different mass and metallicity can provide the necessary observational constraints to distinguish between competing treatments of the complex (magneto-)hydrodynamic processes, which are not fully understood from first principles. Moreover, such observational constraints may guide further refinements of theory.

[1] In the following we consider the region at distances shorter than $\sim$1 kpc (and $\pm$500 pc in Galactocentric direction) as solar neighbourhood in order to minimise bias due to Galactic abundance gradients, see Fig. 1 in Przybilla et al. (2008e) for a schematic representation. This encompasses, in particular, Gould's Belt.

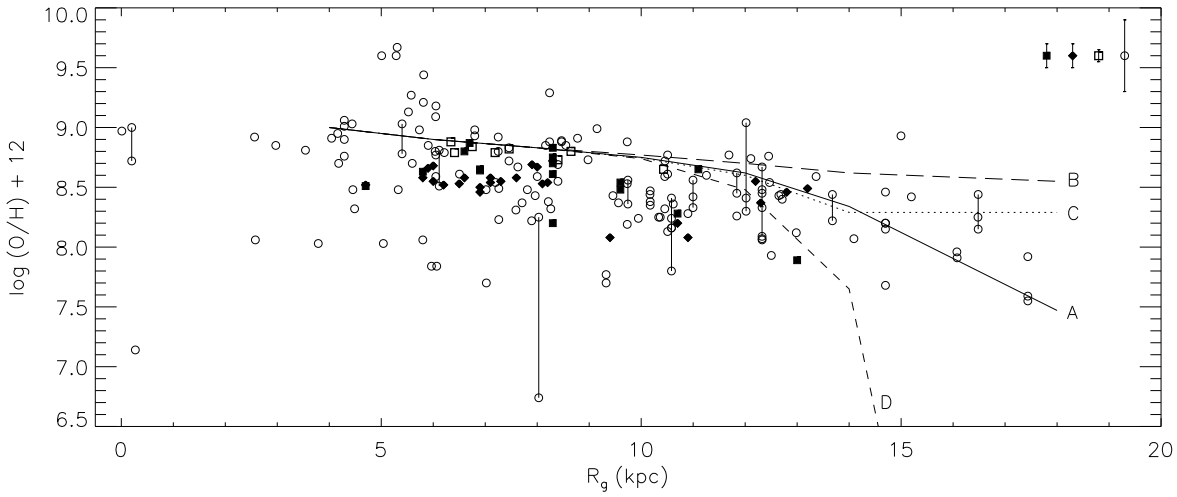

Figure 1.1: Comparison of Galactochemical evolution models (A-D, see Chiappini et al. 2001 for details) with oxygen abundance determinations from H II regions (Esteban et al. 2005: boxes; Rudolph et al. 2006, and references therein: circles) and OB-type stars (Gummersbach et al. 1998: filled boxes; Daflon & Cunha 2004: diamonds), as a function of Galactocentric radius $R_{\rm g}$. The data indicate the existence of an abundance gradient. Note, however, a systematic offset of the mean observed abundances relative to the model and the enormous spread of the observational data, by $\gtrsim$1 order of magnitude at almost any $R_{\rm g}$. Typical error bars are shown in the upper right corner. Symbols are interconnected in cases of double observations. All $R_{\rm g}$ are scaled to a solar Galactocentric distance of $R_0 = 8.0$ kpc (Reid 1993).

However, deriving accurate observational constraints on stellar and Galactochemical evolution is not simple. Most of the quantitative information in astronomy comes from spectroscopy. The information cannot be inferred directly from observation. One has to rely on the interpretation of radiation from light-emitting plasmas, and its interaction with matter, i.e. *quantitative spectroscopy*. Accurate physical modelling is crucial, with systematic uncertainties often dominating the error budget.

Well-understood astrophysical indicators that can contribute to our understanding of stellar and Galactochemical evolution in equal measure are most valuable. Such indicators must meet several criteria: I) they have to be highly luminous in order to be observable over large distances to sample different environments in the universe; II) they should exhibit the spectral features required to address the key questions posed by the cosmic cycle of matter; III) the analysis methods for these indicators should be essentially free of systematic uncertainties. Dwarfs and giants of late O and early B-type (OB-type stars) are in principle such indicators, and even more so their evolved progeny, the supergiants of spectral types B and A.

OB-type Stars. The advantage of OB-type dwarfs and giants lies in their simple atmospheres in radiative equilibrium, which, in combination with insignificant mass-loss, makes the modelling easy in principle. Their spectra exhibit signatures of the light elements, most of the α-process elements, and iron, i.e. many of the astrophysically interesting metal species are accessible. Pristine elemental abundances (unaffected by mixing with nuclear-processed matter or by dust formation and subsequent depletion on dust grains as in the case of H II regions) can be derived only from these unevolved objects. However, large bolometric corrections limit ground-based high-resolution spectroscopy with the available telescopes to objects in the Milky Way and the Magellanic Clouds (MCs).

Numerous abundance studies of early-type dwarfs and giants in the solar neighbourhood have been performed (among the more recent e.g. Gies & Lambert 1992; Kilian 1992, 1994; Cunha & Lambert 1994; Daflon et al. 1999, 2001a,b; Lyubimkov et al. 2005). The early-type stars imply sub-solar present-day abundances[2] on the mean and a large range in abundance of $\sim$1 order of magnitude (see Sect. 4 for more details). Even within individual star clusters/associations the range in derived abundances can reach a factor $\sim$3-5, e.g. in the Orion association and its sub-groups (Cunha & Lambert 1994). A high degree of *chemical inhomogeneity* is indicated for the matter in the solar neighbourhood. This is in contrast to other observational indicators which imply *chemical homogeneity*, like the gas-phase ISM (e.g. Sofia & Meyer 2001; Sofia 2004, and references therein), and to theory, which predicts efficient homogenisation of the ISM through turbulent mixing (Edmunds 1975; Roy & Kunth 1995). Some of the discrepancy is certainly related to differences in atmospheric parameters derived by the various authors for individual objects. These can amount to more than 15% in effective temperature $T_{\rm eff}$ and $\sim$0.5 dex in surface gravity $\log g$ *for the same objects*.

The literature on present-day abundances from H II regions and early-type stars throughout the Galactic disk is too vast to be discussed in detail here. A selective but illustrative summary on the state-of-the-art is given in Fig. 1 (for oxygen; similar trends are derived for other elements). Observation indicates the presence of a relatively steep abundance gradient and a remarkable range in abundance at any Galactocentric distance $R_{\rm g}$. The abundances vary by $\gtrsim$1 order in magnitude, as in the solar neighbourhood. Individual stars in more distant clusters also show a scatter in abundances by factors $\sim$3-5 (e.g. Hunter et al. 2007; Trundle et al. 2007). Moreover, a systematic offset between observed and predicted mean abundances at every $R_{\rm g}$ exists.

Finally, unevolved early-type stars are prominent among the so-called *hyper-velocity stars*, objects moving so fast that they will escape from the Milky Way into intergalactic space. Here, high-precision surface abundance determinations can be used to trace the place of origin of the hyper-velocity stars, see Sect. 5.

BA-type Supergiants. OB-type stars develop to supergiants of late B and A-type (BA-type supergiants, BA-SGs) in a later stage of evolution. These are of particular interest for ground-based observations because of their low bolometric corrections. Thus, BA-type supergiants are among the visually brightest normal stars in spiral and irregular galaxies. At absolute visual magnitudes up to $M_V \simeq -9.5$ they can rival entire globular clusters and even dwarf spheroidal galaxies in integrated light. Consequently, the present generation of 8-10m-class telescopes and efficient instrumentation allows high-resolution spectroscopy of individual BA-type supergiants in the galaxies of the Local Group to be performed. At medium resolution this can potentially be done even in systems out to distances of the Virgo and Fornax clusters of galaxies (e.g. Kudritzki 1998). This would make all classes of late-type galaxies in the Hubble sequence accessible to detailed studies – in the field, in galaxy groups and in clusters.

The spectra of BA-type supergiants extend the chemical species traced by OB-type stars to the entire iron group and additionally s-process elements, thus covering many of the indicators relevant for understanding cosmic nucleosynthesis. These include, but also largely extend the species traced by gaseous nebulae – in particular H II-regions –, the classical abundance indicators in extragalactic research (see e.g. Garnett 2004). Hence, BA-type supergiants can be used to investigate abundance patterns and gradients in other galaxies to a far greater extent than from the study of gaseous nebulae alone. Thus, in general, crucial observational constraints for theoretical investigations of galactochemical evolution can

[2] A reduction of the discrepancies is found if the revised solar abundance standard from hydrodynamic 3-D modelling of the solar atmosphere (Asplund et al. 2005) is adopted instead of earlier work (e.g. Grevesse & Sauval 1998).

be derived. In parallel, the metallicity-dependence of stellar winds and stellar evolution can be studied. Finally, BA-type supergiants can act as primary indicators for the cosmic distance scale by application of the wind momentum–luminosity relationship (WLR, Puls et al. 1996; Kudritzki et al. 1999) and by the flux-weighted gravity–luminosity relationship (FGLR, Kudritzki et al. 2003, 2008; Kudritzki & Przybilla 2003), see Sect. 6. In addition to the stellar metallicity, interstellar reddening and extinction can also be accurately determined, so that BA-type supergiants provide significant advantages compared to classical (photometric) distance indicators such as Cepheid and RR Lyrae stars.

Despite this immense potential, quantitative analyses of BA-SGs are scarce. Only a few of the brightest Galactic objects were studied in an early phase, e.g. Deneb in a pioneering work by Groth (1961) or η Leo (Przybylski 1969; Wolf 1971). The potential of BA-SGs for extragalactic research was already recognised in the first analyses of the visually brightest stars in the Magellanic Clouds (e.g. Przybylski 1968, 1972; Wolf 1972, 1973). These studies were outstanding for their time, but also restricted from the present point of view because of simplified model atmospheres, limited accuracy of atomic data, and the lower quality of the observational material (photographic plates). Note, however, that non-LTE model atmospheres were already investigated at that time (Kudritzki 1973).

BA-type supergiants have become an active field of research again only recently. Venn (1995a,b), Verdugo et al. (1999) and Takeda & Takada-Hidai (2000, and references therein) conducted systematic studies of larger samples of Galactic BA-type supergiants. Stellar parameters and elemental abundances were derived on the basis of hydrostatic line-blanketed LTE model atmospheres, utilising non-LTE line-formation calculations for key ions in some cases. In general, near-solar abundances were found for the heavier elements, resulting in agreement with present-day abundances derived from unevolved Galactic B-stars. Furthermore, the studies indicated (partial) mixing of the surface layers with CN-cycled gas from the stellar core. However, the uncertainties were often quite large. Discrepancies of up to $\sim$20% in $T_{\rm eff}$, $\sim$0.5 dex in $\log g$ and $\sim$1 dex in the elemental abundances can be found for individual objects analysed by different authors. A considerable mismatch between observed and model spectra persisted even for the hydrogen line spectrum when hydrodynamic line-blanketed non-LTE model atmospheres were applied, as in the pilot study on Deneb by Aufdenberg et al. (2002).

Apparently, the quantitative spectroscopy of both – unevolved OB-stars and BA-type supergiants – requires substantial improvements before one can exploit their full potential. This was the motivation for our own efforts. The present work is divided in two parts. Part 1 highlights the main problems and major achievements, and puts several so far unpublished results into the context. The essence of the work in progress is summarised in Figs. 3.1, 4.1, 4.2 and 4.3. Part 2 (the Appendix) summarises our original publications of relevance for the discussion. Note that we have also used our models and analysis methodology with great success for quantitative studies of main sequence A-stars, subluminous B-stars, extreme helium stars, the Sun and solar-type stars. The general outline of Part 1 is as follows. Diagnostic challenges for the quantitative spectroscopy of massive stars are discussed in Sect. 2. The focus is on our improvements in the modelling and in the analysis methodology. Part of the work was accomplished as mentor of the Diploma and PhD projects of Markus Firnstein and Florian Schiller, and of the PhD thesis of Maria Fernanda Nieva. Then, an overview of the present status of our work on the derivation of observational constraints on stellar and Galactochemical evolution is provided in Sects. 3 and 4. Results in the context of hyper-velocity stars are discussed in Sect. 5. Finally, an outlook is given in Sect. 6 on how the studies can be extended in the framework of the young discipline of extragalactic stellar astronomy to achieve a global understanding of the cosmic cycle of matter, and in particular of galactic evolution.

2 Quantitative Spectroscopy

2.1 Observations

The quality of the observational data is one factor that determines the accuracy that can be achieved in quantitative analyses. Because of their brightness, high-resolution spectroscopy of Galactic OB-stars and of BA-type supergiants out to the Magellanic Clouds can be accomplished using 2m-class telescopes. Echelle spectrographs like FEROS on the Max-Planck-ESO 2.2m (Kaufer et al. 1999) or FOCES on the Calar Alto 2.2m telescope (Pfeiffer et al. 1998) are the preferred instruments as they allow all diagnostic lines, which are often scattered throughout the entire optical and near-IR range, to be accessed at once. Moreover, even metal line profiles can be resolved, e.g. for slowly-rotating supergiants. Spectra of bright targets can be obtained at very high signal-to-noise ratios of several hundreds. Such data are required for a *calibration* of the models (see Sect. 2.2), that will later be used for the analysis of larger samples of stars, where a $S/N \lesssim 200$ is sufficient. Careful data reduction beyond standard pipeline applications ensures that line profiles – including in particular the broad hydrogen features – are recovered accurately, which can be verified by comparison with long slit spectra.

Examples of the quality achieved for the spectra used in the calibration of our models and for establishing the analysis methodology are shown in Figs. 2.1 and 2.2 for B-stars and BA-type supergiants, respectively. A good sampling of the parameter space, effective temperature $T_{\rm eff}$ and surface gravity $\log g$, is required for a reliable calibration. Only then can the systematic behaviour of the diagnostic indicators be studied, such as the Stark-broadened hydrogen lines, ionization equilibria (among others e.g. He I/II, C II/III/IV or Si II/III/IV in early B-stars) or various metal features for abundance studies.

Symmetric absorption lines indicate that the photospheres of the stars under study are (close to) hydrostatic. A clear signature of hydrodynamic phenomena is found only in the most luminous supergiants, restricted largely to Hα, which traces the entire stellar atmosphere because of its strength. The line develops from symmetric absorption into a P-Cygni-profile because of the strengthening stellar wind with increasing luminosity.

Fainter objects, like early-type main sequence stars in the Magellanic Clouds or supergiants in more distant Local Group galaxies, require observations with 8-10m-class telescopes. Echelle spectrographs like UVES (Dekker et al. 2000) on the ESO VLT or HIRES (Vogt et al. 1994) and ESI (Sheinis et al. 2002) on Keck are the work horses in this case. However, several hours of observing time per target restrict studies to small samples of stars. Multi-object spectrographs allow these restrictions to be overcome. Instruments like FLAMES/GIRAFFE (Pasquini et al. 2000) on the VLT or DEIMOS (Faber et al. 2003) on Keck provide a multiplex factor of $\sim$100 for a wide field-of-view at a resolving power of $R = \lambda/\Delta\lambda \approx 5000$–$15\,000$, still sufficient for detailed analyses (see Fig. 2.3). At larger distances, in galaxies beyond the Local Group, multi-object spectroscopy of even the most luminous supergiants is feasible only at low to intermediate resolution ($R \approx$1000–2000) at present. FORS1/2 (Seifert et

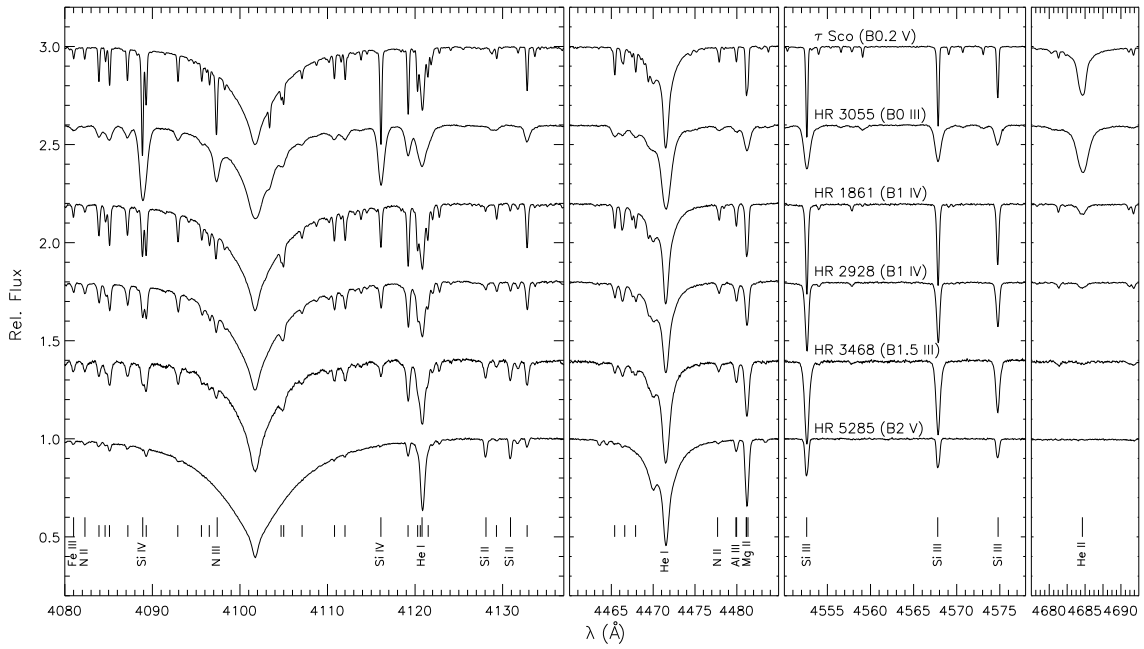

Figure 2.1: Spectral morphology of Galactic B-stars around Hδ, He I λ4471, the Si III triplet $\lambda\lambda$4552–74 and He II λ4686 Å, arranged in a $T_{\rm eff}$ sequence. The major spectral features are identified, short vertical marks indicate O II lines. From Nieva (2007).

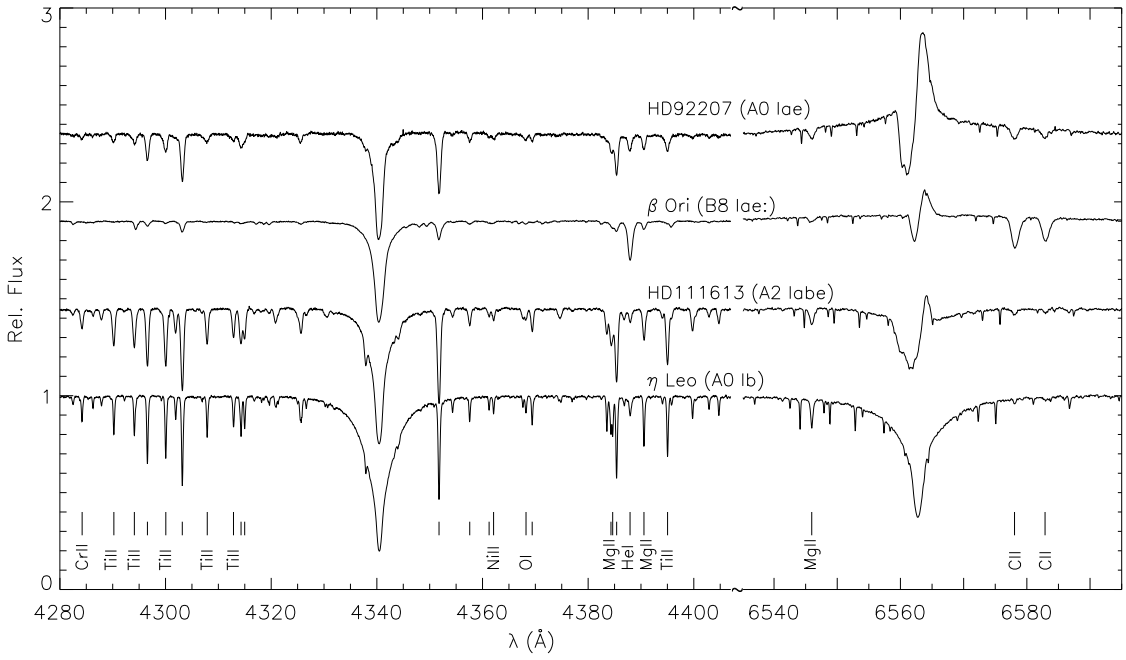

Figure 2.2: Morphology of Galactic BA-type supergiant spectra in regions around Hγ and Hα, arranged in luminosity sequence. The major spectral features are identified, short vertical marks indicate Fe II lines. From Przybilla et al. (2006a).

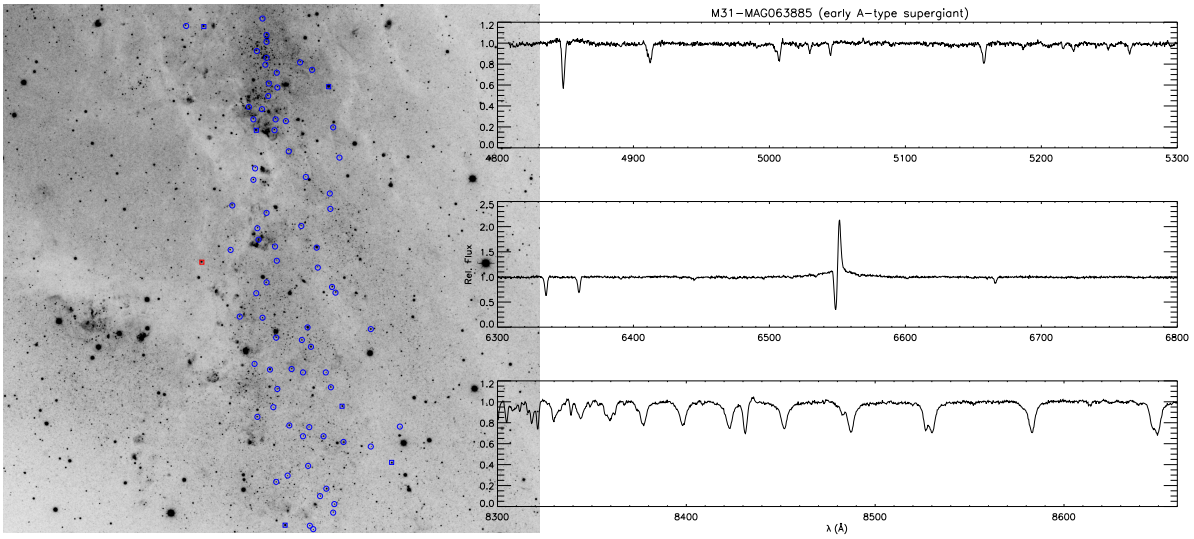

Figure 2.3: Intermediate resolution multiobject-spectroscopy of blue supergiant candidates around the prominent star association NGC 206 in M 31 (V band image with targets marked by blue circles) using DEIMOS on Keck II. Three wavelength regions (around 5000 Å, Hα and the higher Paschen series) of an early A-type supergiant spectrum are shown.

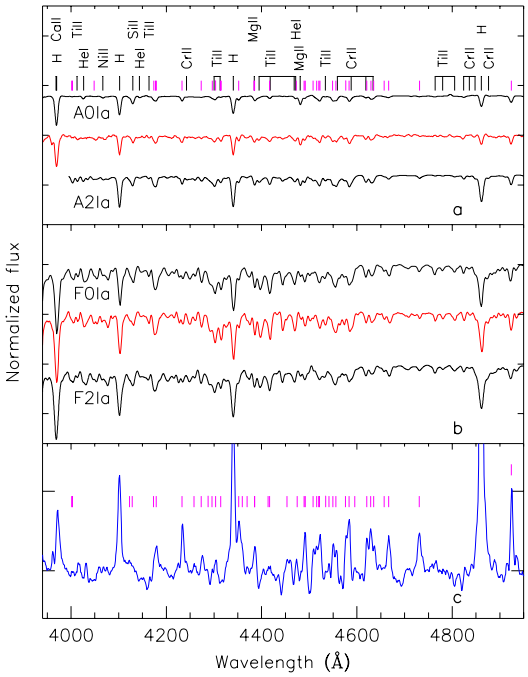

Figure 2.4: Examples of continuum-normalised stellar spectra obtained in NGC 3621, displayed along with Galactic supergiant stars of similar spectral morphology at the same spectral resolution. Ordinate ticks are spaced by 0.5 continuum units. (a) An early A-type supergiant (red line), bracketed by Galactic A0 Ia and A2 Ia template spectra (black). Line identification for the strongest features is shown at the top (unlabelled shorter marks are used for Fe II lines). (b) An early F-type supergiant (red line) compared with Galactic F0 Ia and F2 Ia template spectra (black lines). (c) An LBV candidate. Notice the prominence of several Fe II emission features (identified by the vertical marks) and the presence of nebular emission, indicated by the hydrogen Balmer lines in emission. From Bresolin et al. (2001).

al. 2000) on the VLT has been successfully employed out to distances of several Mpc, like for supergiants at $V \approx 20$–21.5 mag in the field galaxy NGC 3621 (exposing for $\sim$11 hrs in total), see Fig. 2.4.

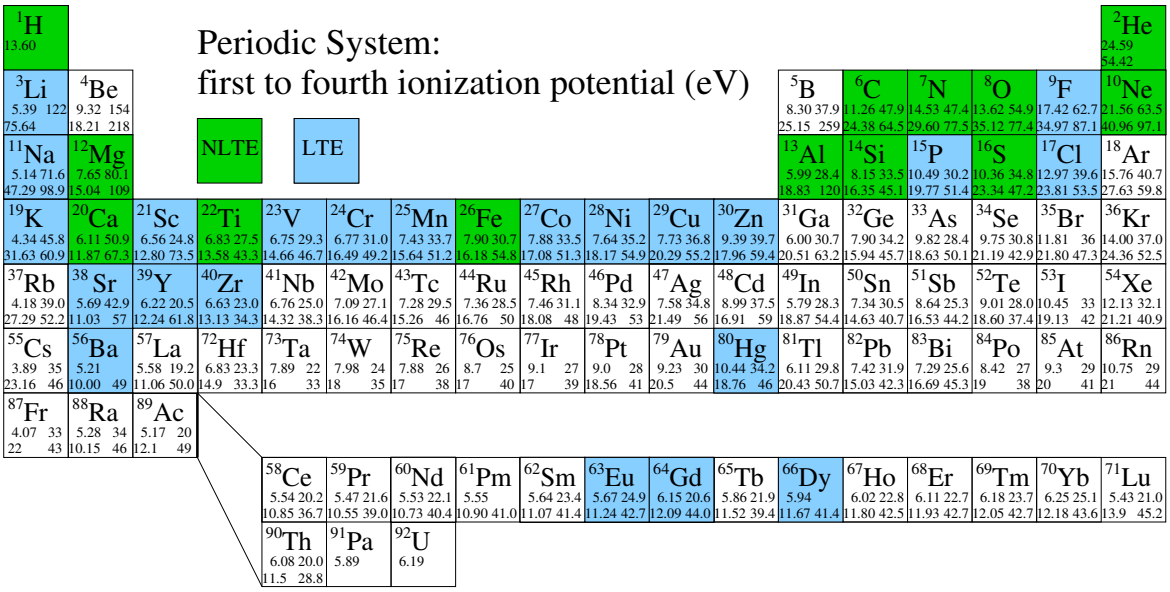

Figure 2.5: Schematic periodic system, indicating the current status of the spectrum synthesis computations with DETAIL/SURFACE. Elements which are implemented in non-LTE are marked in green (see Table 2.1), those in LTE in blue. For each element, the first to fourth ionization potential (in eV, Cox 2000; NIST) is given.

Table 2.1: Non-LTE model atoms for use with DETAIL/SURFACE

Ion	Source	Ion	Source
H	Przybilla & Butler (2004a)	Mg I/II	Przybilla et al. (2001a)
He I/II	Przybilla (2005)	Al III	Dufton et al. (1986)
C I	Przybilla et al. (2001b)	Si II/III/IV	Przybilla & Butler (in prep.)
C II/III/IV	Nieva & Przybilla (2006, 2008)	S II/III	Vrancken et al. (1996), updated
N I/II	Przybilla & Butler (2001)	Ca I/II	Mashonkina et al. (2007)
O I	Przybilla et al. (2000)	Ti II	Becker (1998)
O II	Becker & Butler (1988), updated	Fe II	Becker (1998)
Ne I/II	Butler (in prep.)	Fe III	Butler (in prep.)

2.2 Models & Analysis Methodology

Quantitative spectroscopy of stars relies on model atmospheres. Ideally, these would account for deviations from local thermodynamic equilibrium (non-LTE effects), line blanketing, spherical extension of the atmosphere and for mass outflow in a comprehensive way, refraining from (almost) any approximation. Such models are in principle available (e.g. via the code CMFGEN, Hillier & Miller 1998), but they are computationally so expensive that a mass-production of models as required for the analysis of larger star samples is still beyond present capabilities. However, in practice such sophisticated models are not required for studies of the photospheres of OB-type dwarfs/giants and BA-type supergiants, as simpler approaches turn out to be equivalent in most aspects (Przybilla et al. 2006a; Nieva & Przybilla 2007).

We employ a hybrid non-LTE technique, i.e. non-LTE line-formation calculations on the basis of line-blanketed LTE model atmospheres that assume plane-parallel geometry, chemical homogeneity plus hydrostatic and radiative equilibrium. Model atmospheres are computed with the ATLAS9 code

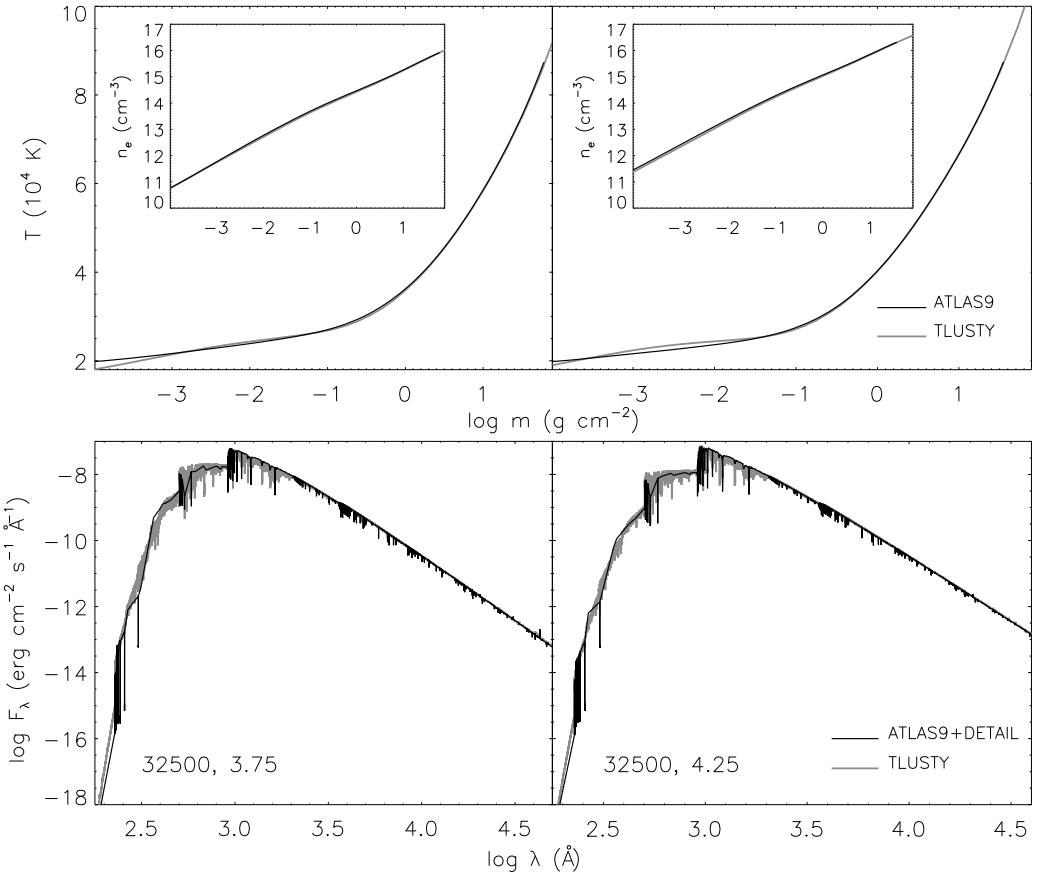

Figure 2.6: Upper panel: Comparison of LTE (ATLAS9) and non-LTE (TLUSTY) model atmosphere structures: temperature and electron density (inset) as a function of column mass for an early B-type dwarf and giant model ($T_{\rm eff}$ and $\log g$ as indicated). Overall, excellent agreement of the model atmospheres is found. The temperature structures deviate by less than 1% in the inner atmosphere, including the regions where the weaker lines and the wings of the stronger features are formed (at column mass $\log m \gtrsim -1$). At the formation depths of the cores of the stronger H and He lines ($-3 \lesssim \log m \lesssim -1.5$) the differences may increase to $\lesssim$ 2–3%. Larger deviations may occur only in the outermost parts of the atmosphere, outside the line-formation depths. Lower panel: Comparison of spectral energy distributions, the radiation field computed by DETAIL on the basis of the ATLAS9 atmospheric structure vs. TLUSTY. Excellent agreement is obtained throughout practically the entire wavelength range. Both comparisons together indicate the hybrid non-LTE approach to be equivalent to full non-LTE calculations for this kind of star. From Nieva & Przybilla (2007).

(Kurucz 1993). The non-LTE line-formation package DETAIL/SURFACE (Giddings 1981; Butler & Giddings 1985; both updated by K. Butler) is used to address the restricted non-LTE problem. The coupled radiative transfer and statistical equilibrium equations are solved with DETAIL, employing the Accelerated Lambda Iteration scheme of Rybicki & Hummer (1991). This allows even complex ions to be treated in a realistic way, see Table 2.1 for a summary of model atoms used with DETAIL in this context. Synthetic spectra are calculated on the basis of the resulting level populations with SURFACE, using refined line-broadening theories. Alternatively, the formal solution can also be performed with SURFACE in LTE, see Fig. 2.5 for an overview of implemented models.

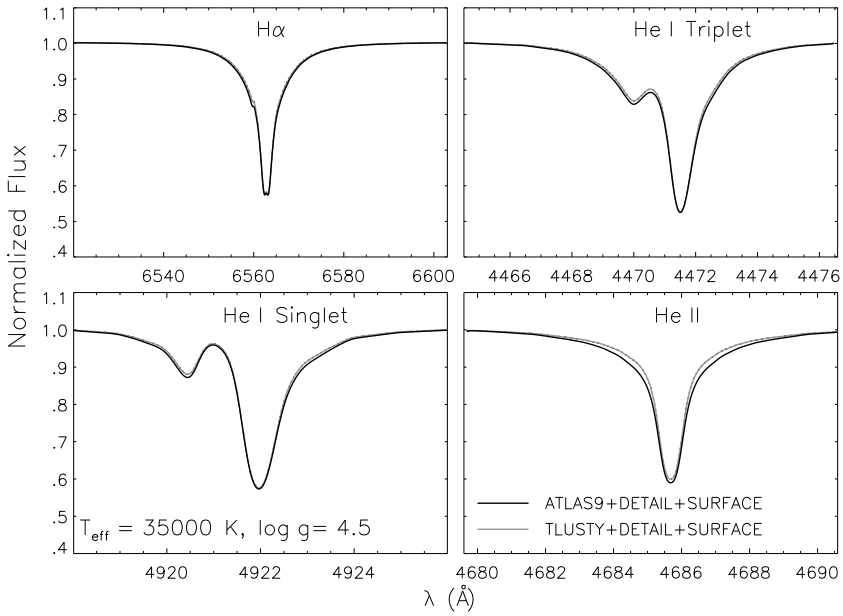

Figure 2.7: Comparison of the most discrepant hydrogen and He I/II line profiles from our hybrid non-LTE approach – using an ATLAS9 model atmosphere (LTE) plus non-LTE line-formation with DETAIL/SURFACE – and a calculation using the corresponding TLUSTY model atmosphere (non-LTE) plus non-LTE line-formation with DETAIL/SURFACE for a hot main sequence model. Practically perfect agreement is obtained, with small discrepancies occurring only in the wings of He II λ4686 Å. This is another example for the equivalence of our hybrid non-LTE approach and full non-LTE calculations, this time from the viewpoint of detailed line profiles. From Nieva & Przybilla (2007).

Several conditions need to be met in order to determine reliable level populations (a prerequisite for an accurate analysis) from the solution of the radiative transfer and statistical equilibrium equations (see e.g. Mihalas 1978): I) the local temperatures and particle densities have to be known (i.e. the atmospheric structure) *and* II) the radiation field has to be realistic *and* III) all relevant atomic processes have to be taken into account *and* IV) high-quality atomic data have to be available (i.e. accurate cross-sections for the transitions). In particular, I) and II) require a realistic physical model of the stellar atmosphere and an accurate atmospheric parameter determination. Items III) and IV) are related to the model atoms, i.e. the specifications of atomic input data to be considered in the non-LTE calculations. Shortcomings in any of I)–IV) result in increased uncertainties/errors of the analysis.

Extensive tests have been made to verify the validity of our modelling assumptions in terms of items I) and II) above. One example is shown in Fig. 2.6, where a comparison of our approach with full non-LTE models (Lanz & Hubeny 2003) in the OB-star regime is made. Excellent agreement is found for the atmospheric structures and spectral energy distributions, indicating the equivalence of both approaches, see Nieva & Przybilla (2007) for details. This is corroborated further by a comparison of the resulting line profiles of the hydrogen and helium spectra, see Figs. 2.7 and 2.8. The comparison with observation shows that our hybrid non-LTE approach allows the best match to be obtained, outperforming the other models discussed in Fig. 2.8. Similar tests have been made for BA-type supergiants (Przybilla 2002; Przybilla et al. 2006a). Good agreement with model predictions from the unified (wind+photosphere) non-LTE code FASTWIND (Puls et al. 2005) is found for this kind of star. Deviations can also occur for metal lines. However, this is mostly due to *different model atoms used in the various codes*.

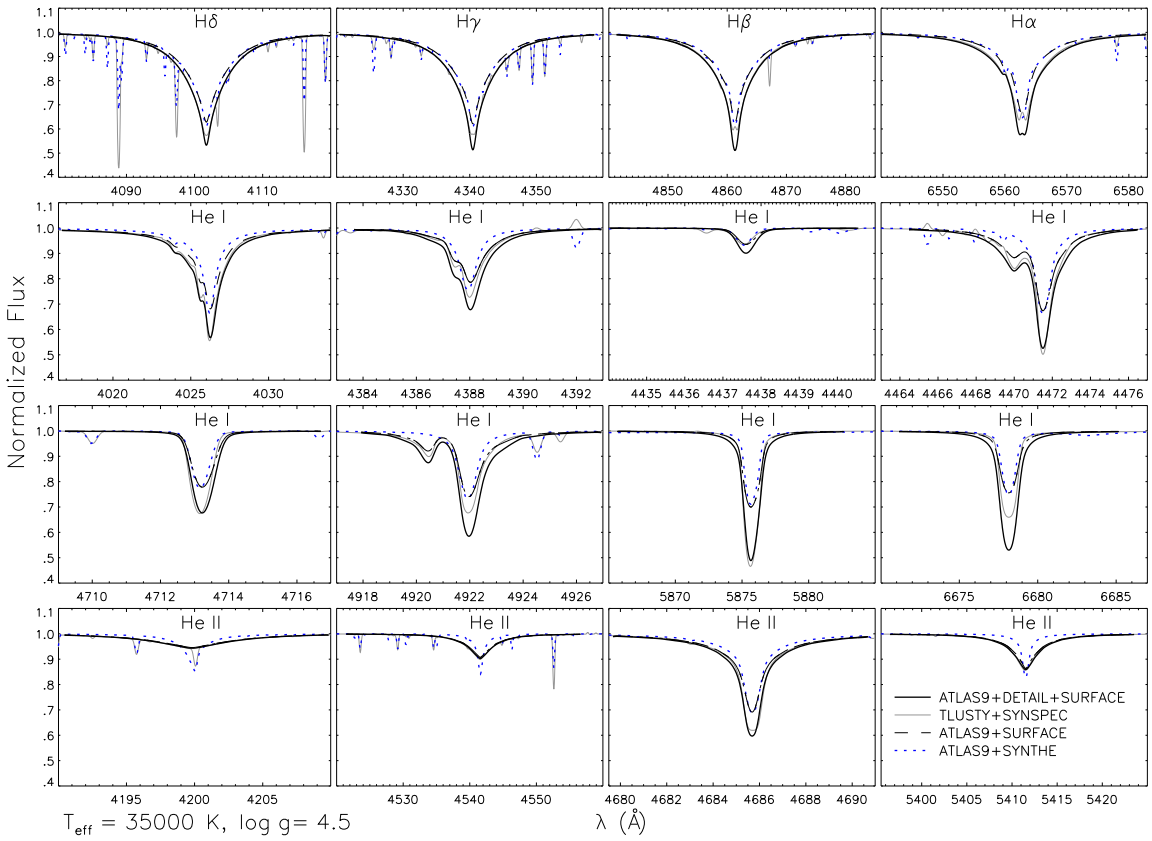

Figure 2.8: Comparison of selected hydrogen and He I/II line profiles from our hybrid non-LTE approach (using ATLAS9+DETAIL/SURFACE), non-LTE computations with TLUSTY+SYNSPEC and two LTE calculations (ATLAS9+SURFACE and ATLAS9+SYNTHE) for the same hot main sequence model as discussed in Fig. 2.7. I) ATLAS9+DETAIL/SURFACE vs. TLUSTY+SYNSPEC: Notable differences between both solutions occur in the line cores of the Balmer lines (the latter are filled in by emission) and in the He I singlet lines, which are systematically weaker in the latter case. The He I triplet lines on the other hand agree much better. Small discrepancies occur in the line wings of the He I lines because of different broadening data. A good match is also obtained for the He II lines, with small differences arising in He II λ4686 Å. This needs to be compared to observation, see Fig. 4 of Nieva & Przybilla (2007) for the closest analogue: our hybrid non-LTE approach is favoured, TLUSTY+SYNSPEC calculations will face difficulties in achieving a fit as good, in particular with regard to all the He I singlet lines. II) ATLAS9+DETAIL/SURFACE vs. LTE calculations: The model predictions obtained with ATLAS9+SYNTHE differ notably in all respects: the lines are not strong enough because of the neglect of non-LTE effects on the level populations and in many cases suffer further from use of inappropriate line-broadening data (in particular for the diffuse He I lines and for He II). LTE computations with ATLAS9+SURFACE improve upon this, while still failing in obtaining a good overall match because of the neglect of non-LTE effects. The comparison with observation is always decisive. Note that metal lines are accounted for only in the TLUSTY+SYNSPEC and ATLAS9+SYNTHE computations. From Nieva & Przybilla (2007).

The importance of *realistic* model atoms for quantitative spectroscopy is largely ignored in contemporary astrophysics. This has many reasons. In the past, development was hampered by the lack of the required atomic data. The situation has changed dramatically over the last two decades by the efforts made within the Opacity Project (OP, e.g. Seaton et al. 1994) and the IRON Project (Hummer

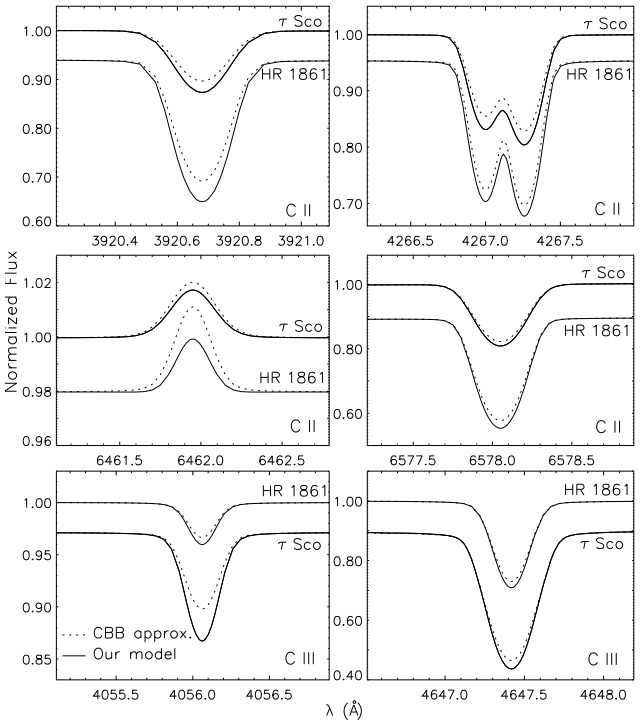

Figure 2.9: Comparison of synthetic C II/III line profiles for two B-type dwarfs (τ Sco, B0.2 V and HR 1861, B1 IV) using different model atoms. One calculation is based on our well-tested reference model including many collisional data from *ab-initio* calculations while the other adopts standard approximations (Van Regemorter 1962; Allen 1973, with collision strength $\Omega = 1$) for evaluating collisional rates for all transitions. Abundance determinations based on the simple model would indicate a significantly larger scatter in the values derived from individual lines. Note that the effects vary from star to star. From Nieva & Przybilla (2008).

et al. 1993), and by many developments published continuously in the atomic physics literature, which, however, draw little attention within the astronomical community.

In fact, the bulk of stellar studies addresses objects that are in general supposed to show small deviations from detailed equilibrium (cool and tepid stars). There appeared little need to invoke non-LTE techniques for quantitative analyses, a credo being dropped only slowly. For the remainder (hot stars), the focus was to include huge amounts of atomic data required for the computation of non-LTE model atmospheres in the most efficient way. Large, uniform databases like those provided by e.g. the OP allowed *simple* model atoms to be constructed (nearly) automatically. In reality, model atmosphere computations do not require an exact treatment of the millions of individual lines. A good approximation of the opacities even in a statistical sense is sufficient, masking (most) shortcomings in model atoms. However, for the comparison with the observed line spectra any simplification/inaccuracy in the atomic data *can* matter.

Non-LTE effects prevail whenever radiative processes – which are *non-local* in character (photons may travel wide distances before interacting with the plasma) – dominate the transition rates. Hence, great care is usually (also in our case) exercised to implement accurate oscillator strengths and photoionization cross-sections in model atoms. On the other hand, collision processes thermalise. Collisions do not obey the restrictive selection rules for radiative transitions. In consequence, many processes, such as the coupling between different spin systems in the lighter elements, are determined by collisional rates. However, homogeneous and comprehensive databases on collisional data for ions relevant for stellar atmospheres are still not available. Therefore, simple approximations are usually made to evaluate collision rates, an assumption too crude for accurate quantitative analyses.

In many cases better data for (mostly) electron-impact excitation cross-sections from *ab-initio* computations exist. A comparison of model predictions accounting for accurate collisional data and for

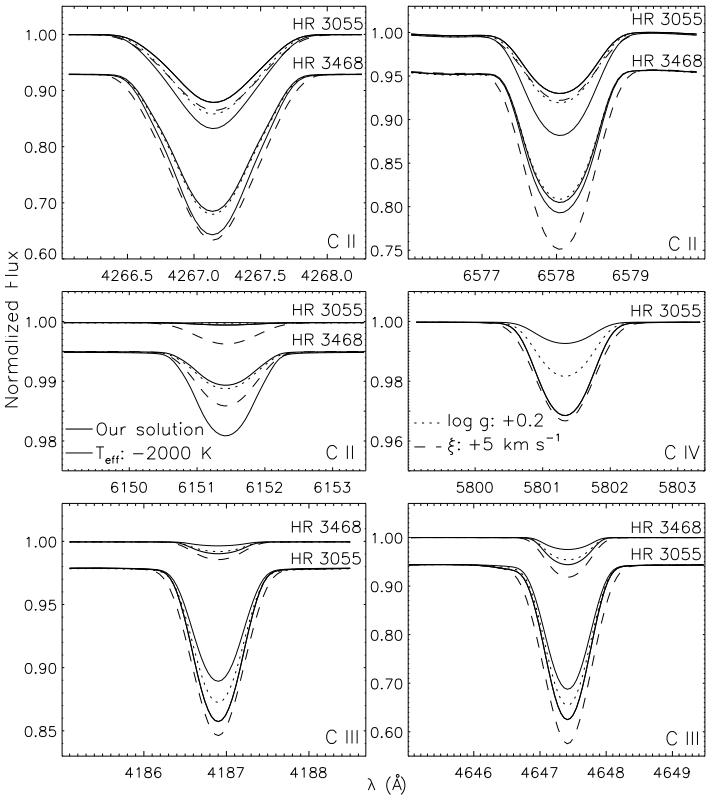

Figure 2.10: Sensitivity of selected C II–IV lines to atmospheric parameter variations (as indicated) in two early B-type giants: HR 3055 (B0 III) and HR 3468 (B1.5 III). Our solution corresponds to the final parameters derived for these stars and a constant C abundance for all lines. The parameter offsets are typical for statistical and systematic uncertainties from published values. All atmospheric parameters need to be constrained well for the ionization equilibria to be established. The star HR 3468 is too cool to show C IV lines. From Nieva & Przybilla (2008).

those using standard approximations in the example of carbon (Fig. 2.9) shows considerable effects on the spectrum synthesis. Note that the effects may vary with the plasma parameters (temperature, density), as these affect the transition rates. In a similar way the extent of the model atom, e.g. the energy levels or transitions considered, can influence the model predictions. Use of radiative data from different sources may also lead to noticeable effects (see e.g. Nieva & Przybilla 2008). Therefore, a comparison with observation (for as many spectral lines as possible) is required to decide which model atom realisation provides the closest match – a procedure called *model atom calibration*. One can take advantage of the rules and regularities of atomic physics for guidance in this process. A wide range of stellar parameters should be considered in the calibration (i.e. stars of different spectral type/luminosity class), as the resulting model atom has to reproduce observation equally well in all objects.

The model atom calibration is complicated by the fact that the stellar parameters of the calibration stars may not be known precisely *a priori*. Examples of the effects of stellar parameter variations on the predicted line profiles are shown in Fig. 2.10 (for details see Nieva & Przybilla 2008). Note that the individual spectral lines react in different ways to the variations. Consequently, the determination of stellar parameters (using methods discussed next) and the model atom calibration have to be done hand in hand, requiring iteration to constrain the entire set of parameters. Fulfilment of boundary conditions, like ionization balance (all ionization stages of an element are required to indicate the same abundance), are of crucial importance in this process. The aim is to minimise the abundance scatter from the analysis of the entire line list, see Fig. 2.11 for an example. This has to be achieved for all calibration stars simultaneously, which makes the process highly complex. However, once calibrated, model atoms like those from Table 2.1 are available for accurate quantitative analyses forthwith.

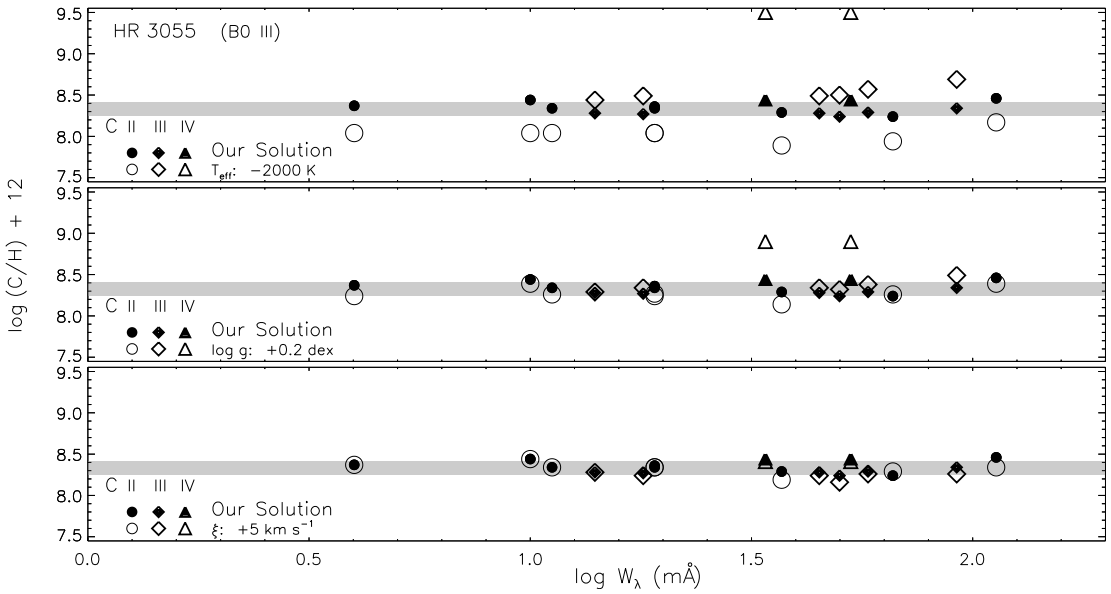

Figure 2.11: Sensitivity of carbon abundances to stellar parameter variations (for HR 3055, B0 III): $T_{\rm eff}$ (upper), $\log\ g$ (middle) and microturbulent velocity ξ (lower panel). The offsets of the parameters are displayed in the lower left part of each panel. A large spread in abundance from individual lines of the three ionization stages results, in particular for variations of $T_{\rm eff}$. Note also the implications of using only few lines of one ion for abundance determinations in the presence of systematic errors in the atmospheric parameters. The grey bands correspond to 1σ-uncertainties of the stellar C abundance in our solution. From Nieva & Przybilla (2008).

2.3 Stellar Parameter Determination

Our stellar parameter determination relies on a spectroscopic approach. *Multiple* non-LTE ionization equilibria and all available Stark-broadened hydrogen lines (usually from the Balmer and Paschen series) are used rigorously as temperature and surface gravity indicators, analysed via detailed line-profile fits (χ^2-minimisation). An example of the procedure is shown in Fig. 2.12. Ionization equilibria and the hydrogen lines are both required as the individual indicators are degenerate with respect to simultaneous variations of $T_{\rm eff}$/$\log g$. However, the intersection of the different loci determines the stellar parameters to high accuracy. The uncertainties in $T_{\rm eff}$ can be as low as 1–2% and 0.05–0.10 dex in $\log g$ (Przybilla et al. 2006a; Nieva & Przybilla 2008). The *redundancy* of matching several indicators simultaneously is one of the main improvements and strengths of our approach.

A further improvement is a self-consistent account of 'secondary' parameters, such as helium abundance (all available helium lines are analysed), metallicity (from the abundance determination, see Sect. 2.4) and microturbulence[3], which were either approximated or even ignored for the basic parameter determination in previous studies. These may indeed be of secondary importance for less luminous objects in most cases. However, in particular close to the Eddington limit they can no longer be neglected, as the balance of gravitational forces and radiative acceleration, which strongly impacts the atmospheric structure in supergiants, is delicate (Przybilla et al. 2006a). This complicates the stellar pa-

[3]The microturbulent velocity ξ is determined as usual by demanding elemental abundances to be independent of line equivalent width W_λ. Note that we do not find a need to assume different values of ξ for individual ions (even of the same element, see e.g. Albayrak 2000), or to assume depth-dependent microturbulent velocities.

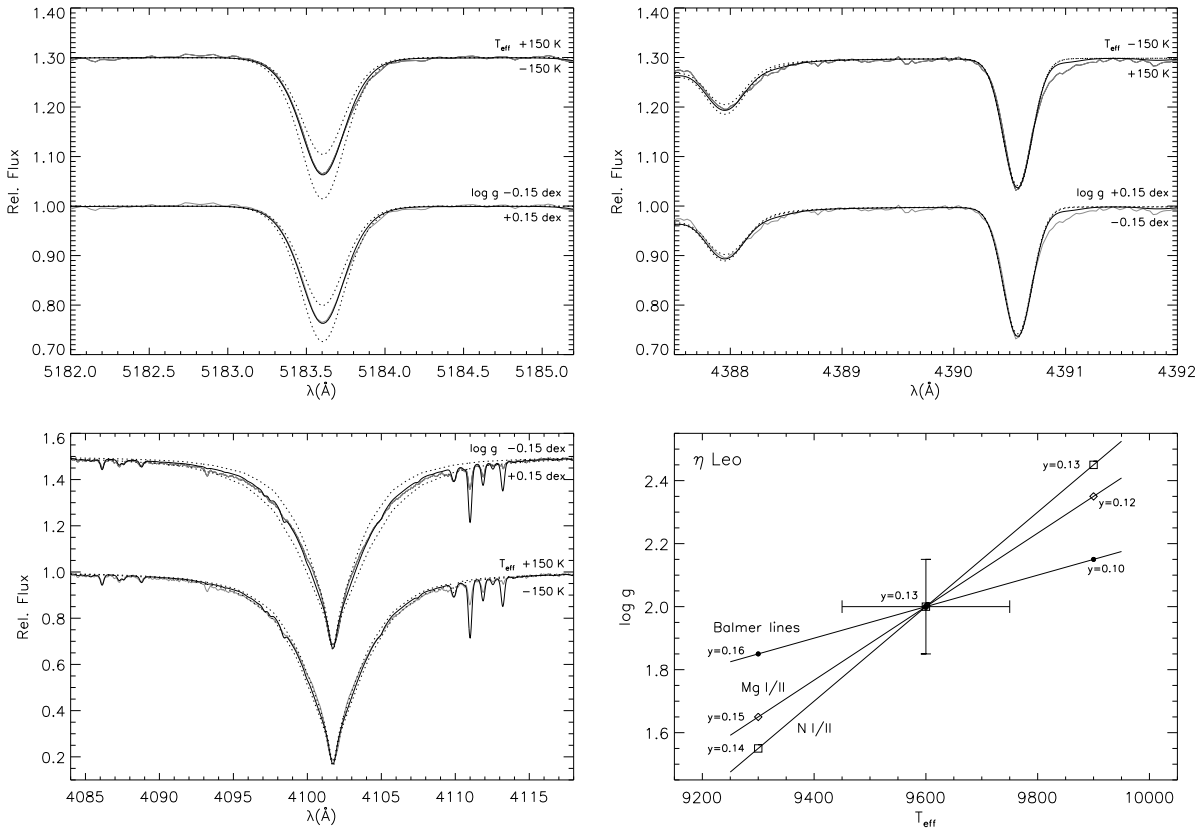

Figure 2.12: Impact of stellar parameter variations (within conservative uncertainties) on non-LTE line profile fits for diagnostic lines in the Galactic A-SG η Leo: ionization equilibrium of Mg I (upper left panel) and Mg II (also including He I λ4388 Å, upper right panel) and the Stark-broadened Hδ line (lower left panel). Spectrum synthesis for the final parameters (thin black line) and varied parameters, as indicated (dotted lines), are compared to observation (grey). Vertical shifts have been applied to the upper profiles. Note the high sensitivity of the minor ionic species Mg I to parameter variations, while Mg II is almost unaffected. Application to the different parameter indicators allows a fit diagram in the $T_{\rm eff} - \log g$-plane to be constructed (lower right panel). The stellar parameters are determined from the intersection of the individual indicators. The curves are parameterised by the helium abundance y. From Przybilla et al. (2006a).

rameter determination enormously, resulting in the need for *iterative* optimisation in a five-dimensional parameter space instead of solving the usual two-dimensional problem (in $T_{\rm eff}$ and $\log g$). The huge differences in basic parameters of BA-type supergiant studies from the literature (see Sect. 1) can be expected, as none of the previous investigations accounted for this in full.

An important cross-check is the comparison with the observed spectral energy distribution (SED), i.e. verifying that not only the diagnostic features in the spectra are matched but also the *global* energy output of the star. Examples for the excellent agreement between our model atmosphere computations and observations for BA-type supergiants and OB-stars are displayed in Fig. 2.13.

Line-profile fitting of high-resolution spectra also allows detailed information on (projected) rotational velocity $v \sin i$ and macroturbulence ζ to be derived. An example is shown in Fig. 2.14. Macroturbulent velocity fields turn out to be widespread among OB-type stars and BA-type supergiants.

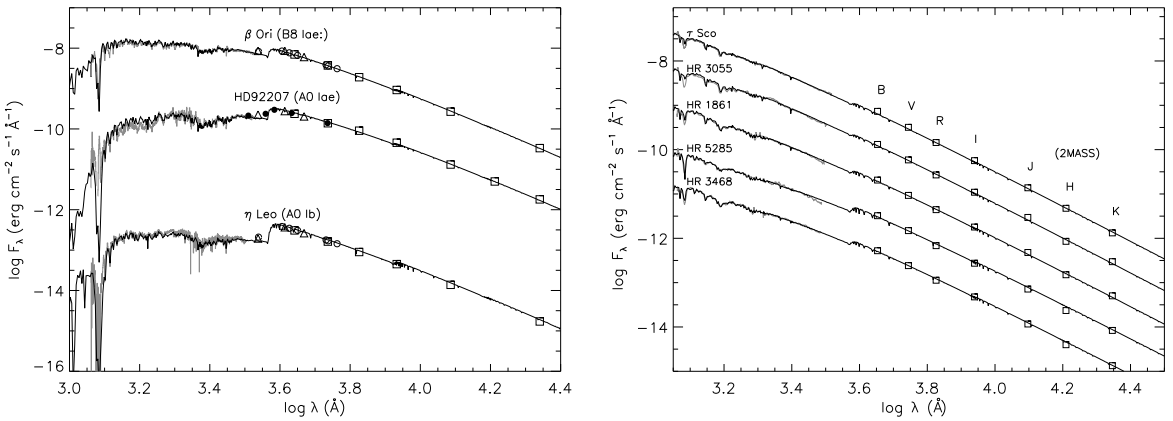

Figure 2.13: Comparison of model fluxes (black lines) and observed SEDs from the UV to the near-IR, for BA-SGs (left panel) and B-type stars (right panel). Displayed are IUE spectrophotometry (grey lines), Johnson (boxes), Strömgren (triangles), Walraven (filled circles) and Geneva photometry (open circles). The observations have been dereddened. From Przybilla et al. (2006a); Nieva & Przybilla (2006).

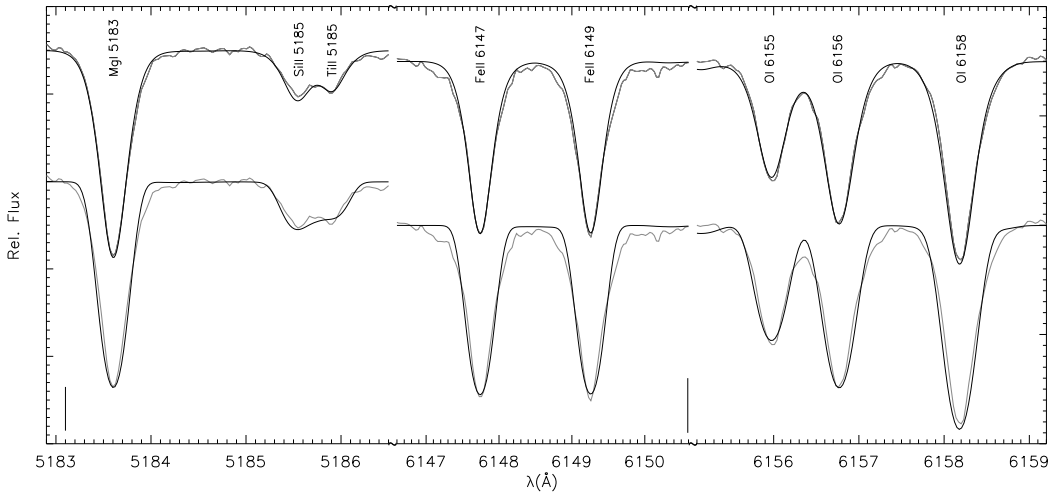

Figure 2.14: Line-profile fits (thin black) to observation of the A-SG η Leo (grey lines) accounting for rotation and macroturbulence (upper comparison) and for rotation only (lower comparison). An excellent match is obtained in the first case. The markers are vertically extended by 0.05 units. From Przybilla et al. (2006a).

Finally, when assembling all information (atmospheric parameters, photometry, comparison with stellar evolution models, etc.), a comprehensive view of the stars under study may be developed. This encompasses in particular the fundamental stellar parameters mass M, luminosity L and radius R.

2.4 Elemental Abundances

The chemical composition can be determined with high precision once accurate atmospheric parameters are available. Again, line-profile fitting is preferred over traditional curve-of-growth techniques for the analysis.

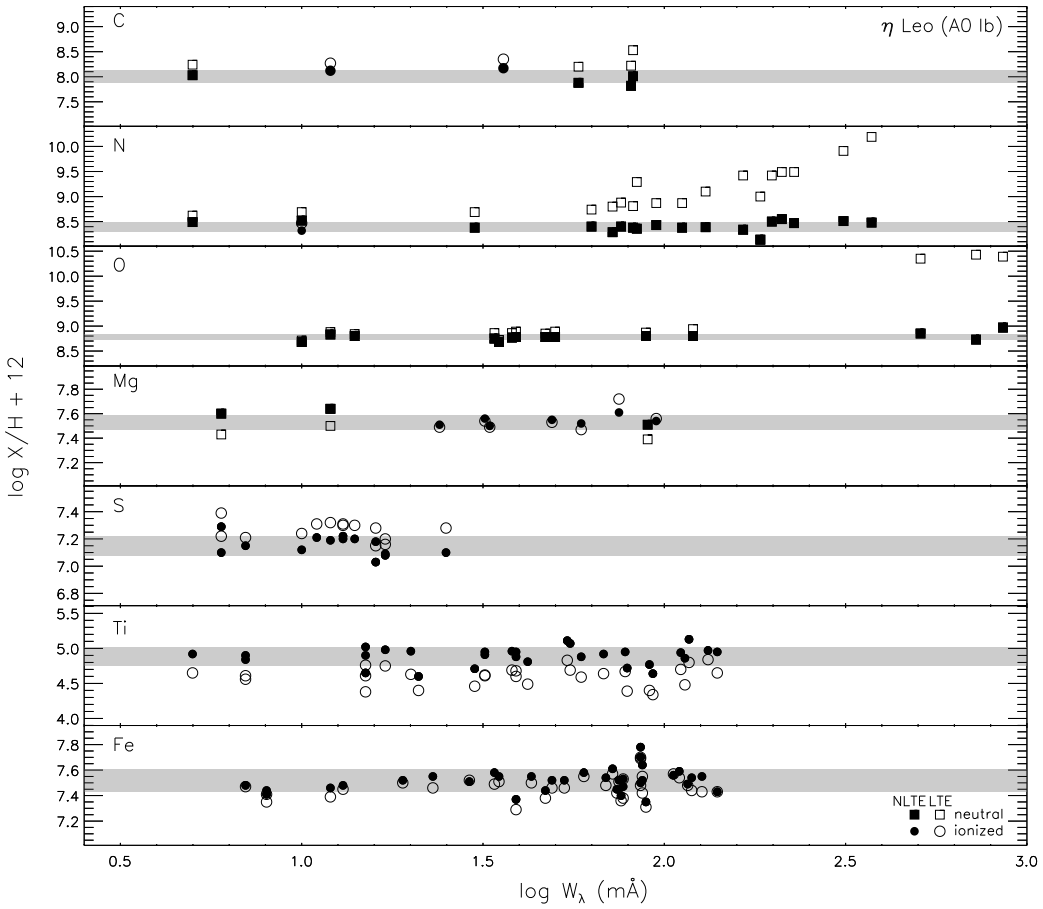

Figure 2.15: Line abundances for several elements in η Leo as a function of equivalent width (see legend for symbol identifications). The grey bands cover the 1σ-uncertainty ranges around the non-LTE mean values. Non-LTE calculations reduce the line-to-line scatter and remove systematic trends. Note that even weak lines can show considerable departures from LTE. From Przybilla et al. (2006a).

An example for the abundance analysis of an A-type supergiant is shown in Fig. 2.15. Homogeneous abundances are derived from *all* lines in the element spectra, which show little scatter around the mean value. Our rigorous non-LTE analysis thus avoids the systematic trends of abundance with line-strength found in the LTE approximation, e.g. for N I or O I. In other cases, for S II, Ti II and Fe II, the non-LTE abundances are systematically shifted relative to LTE. Also the statistical scatter is reduced in non-LTE, and contrary to common assumption significant non-LTE abundance corrections are found even in the weak-line limit. These can exceed a factor $\sim$2 for lines with $W_\lambda \lesssim 10$ mÅ, in particular for more luminous objects, where non-LTE effects are amplified. In addition, systematic errors need to be considered because of uncertainties in the stellar parameters, atomic data, and the quality of the spectra. We find that non-LTE abundance uncertainties amount to typically 0.05–0.10 dex (random) and $\sim$0.10 dex (systematic 1σ-errors) when applying our analysis methodology in combination with realistic model atoms to high-S/N spectra. This applies to OB-stars and BA-type supergiants alike. It is hereby shown that *previously reported problems in reproducing observed spectra are only artefacts of inadequate models and/or analysis techniques*.

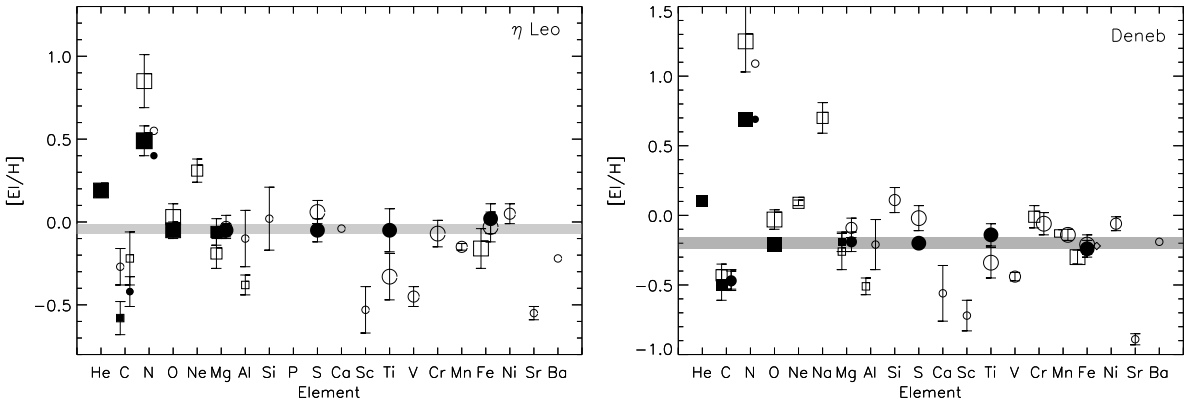

Figure 2.16: Elemental abundance analysis (relative to the solar composition, Grevesse & Sauval 1998) for two bright Galactic A-type supergiants. Symbol identification as in Fig. 2.15, the symbol size codes the number of spectral lines analysed. The error bars represent 1σ-uncertainties from the line-to-line scatter. The grey shaded area marks the deduced metallicity of the objects within 1σ-errors. Non-LTE abundance analyses reveal a (scaled) solar abundance pattern, except for the light elements which have been affected by mixing with nuclear-processed matter. From Przybilla et al. (2006a); Schiller & Przybilla (2008).

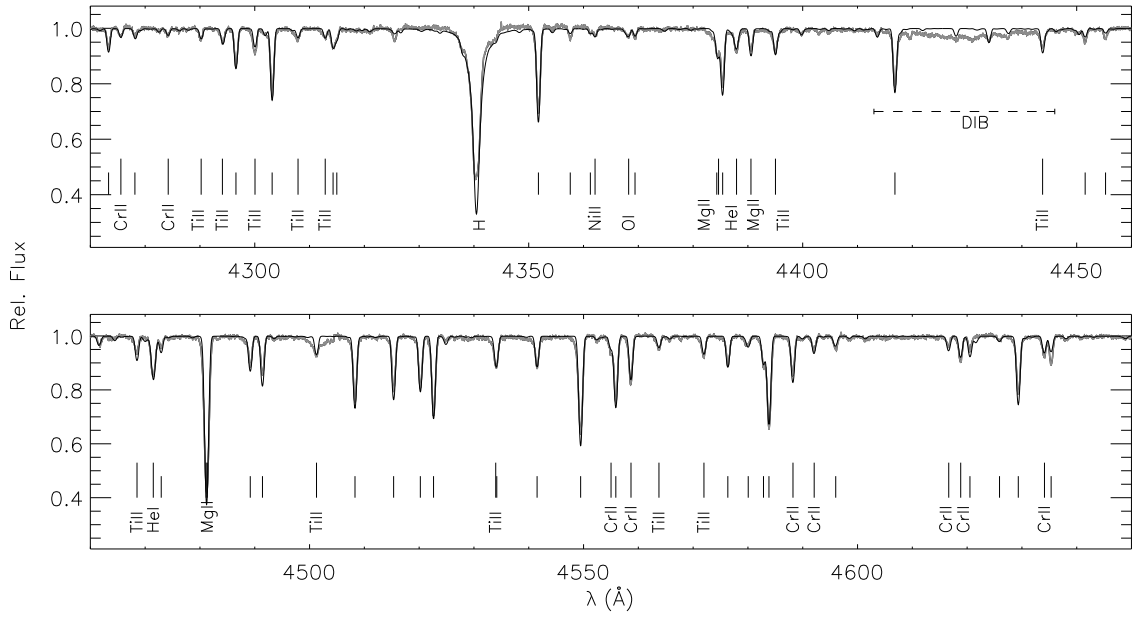

Figure 2.17: Comparison of spectrum synthesis (thin black line) with a high-resolution spectrum of the Galactic A-type supergiant HD 92207 (grey). The major spectral features are identified, short vertical marks designate Fe II lines. The location of the diffuse interstellar band around 4430 Å is indicated. With few exceptions, excellent agreement between theory and observation is found (Hγ is affected by the stellar wind in this highly luminous star). From Przybilla et al. (2006a).

A comprehensive view of abundances in two Galactic high-luminosity A-type supergiants is given in Fig. 2.16. The non-LTE analysis gives a scaled solar composition for the heavier elements, and abundance patterns of the lighter elements characteristic for mixing with CN-processed matter. This is consistent with what is expected for evolved massive Population I stars. Inappropriate LTE analyses on the other hand tend to systematically underestimate iron group abundances and overestimate the light and α-process element abundances by up to factors of 2–3 on the mean (most noticeable in HD 92207). Taking the LTE results at face value this would imply α-enhancement, a characteristic feature of old Population II objects, which, however, is in sharp contrast to the young nature of the supergiants. In other galaxies, where we have less-comprehensive independent information, such LTE analyses may result in misleading conclusions. Note that while many astrophysically important elements are covered by our non-LTE calculations, the investigation of many other species is restricted to LTE in BA-SGs, as model atoms are unavailable at present. Considerable efforts will be required to complete the analysis inventory. On the other hand, model atoms for most observed ions in OB-stars are already available.

The precision achieved in the individual line analysis results in a highly consistent match of the *entire* synthetic spectrum with observation, see e.g. Fig. 2.17. Approximately 70% of the total number of features in the optical and near-IR spectra of BA-type supergiants can be considered in non-LTE at present, and the rest in LTE. The coverage of features that can be treated in non-LTE is over 90% in OB-type stars at these wavelengths, see e.g. Przybilla et al. (2008b) and Fig. 5.1 for examples of the quality that can be achieved in fitting observed spectra.

Such comprehensive spectrum synthesis is a prerequisite for the analysis of medium-resolution spectra, such as provided by multi-object spectrographs. Individual lines can often no longer be resolved in that case. Possible applications include in particular the study of faint objects at larger distances like OB-type main-sequence stars in the Magellanic Clouds or BA-type supergiants in galaxies beyond the Local Group, see Sect. 6 for a discussion.

2.5 Near-IR Spectroscopy

Near-IR observations of early-type stars are a relatively new field to astronomy. They are motivated by the desire to study star formation and young stellar populations throughout the Galactic disk and in the Galactic Centre in particular – regions where strong extinction prohibits observations in the optical. Moreover, the field will grow in importance once the next generation of extremely large telescopes – the 42m-diameter European E-ELT, the 24m Giant Magellan Telescope (GMT) and the Thirty Meter Telescope (TMT) – comes into operation. These will rely on adaptive optics in order to facilitate diffraction-limited observations. As a consequence, they will be operated primarily in the near-IR, limited by technological feasibility and budget constraints.

Little information on quantitative near-IR spectroscopy of normal OB-type dwarfs/giants can be found in modern literature (Lenorzer et al. 2004; Repolust et al. 2005). Even less is known on BA-type supergiants.

Problems with the models were indicated in the pioneering study of the Paschen and in particular the Pfund series in the A-supergiant prototype Deneb (Aufdenberg et al. 2002), which were attributed to deficiencies in our understanding of the physics of stellar atmospheres. It was later shown (Przybilla & Butler 2004a) that this was in fact a result of inaccurate electron-impact excitation cross-sections used in the hydrogen model atom by Aufdenberg et al. (2002). The sensitivity of the near-IR lines of hydrogen to the model assumptions is demonstrated in Fig. 2.18. This is because of the amplification

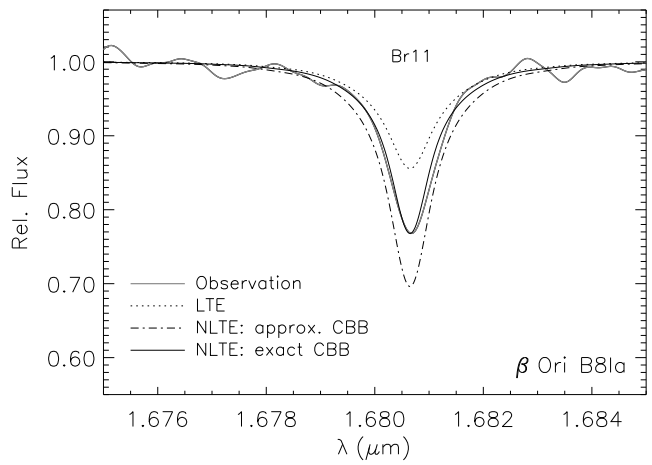

Figure 2.18: Modelling of hydrogen lines in the near-IR, e.g. Br11 in the late B-SG β Ori, using different approaches according to the legend. Agreement between observation and theory can be obtained only in non-LTE when electron-impact excitation data from *ab-initio* calculations are adopted. Non-LTE computations using approximations for the evaluation of collisional bound-bound rates overpredict equivalent widths by a factor $\sim$2 in this case, while LTE modelling gives much too weak lines. Stellar parameters as determined from the analysis in the optical have been adopted. All three models reproduce the higher Balmer lines equally well. From Przybilla & Butler (2004a).

of non-LTE effects in the Rayleigh-Jeans tail of the energy distribution of hot stars. The line source function may be written as

$$S_l = \frac{2h\nu^3/c^2}{b_i/b_j \exp(h\nu/kT) - 1}\,, \tag{2.1}$$

using standard nomenclature for physical constants. The source function is particularly sensitive to variations in the ratio of the departure coefficients b_i

$$\begin{aligned} |\Delta S_l| \quad &= \quad \left| \frac{S_l}{b_i/b_j - \exp(-h\nu/kT)} \Delta(b_i/b_j) \right| \\ &\underset{h\nu/kT \ll 1}{\approx} \quad \left| \frac{S_l}{(b_i/b_j - 1) + h\nu/kT} \Delta(b_i/b_j) \right| \end{aligned} \tag{2.2}$$

when $h\nu/kT$ is small, because the denominator can adopt values close to zero, amplifying effects of a varying $\Delta(b_i/b_j)$. This makes near-IR lines in hot stars very susceptible to even small changes in the atomic data and details of the calculation. In fact, the b_i vary by only several percent in the example in Fig. 2.18, resulting in changes by a factor $\sim$2 in equivalent width. For the particular case of Deneb, an excellent match of model and observation has been obtained in the meantime (Schiller & Przybilla 2008), see Fig. 2.19.

Similar sensitivities to details of the model calculations are also found for helium lines in hot stars (Przybilla 2005; Przybilla et al. 2005; Nieva & Przybilla 2007). Examples are shown in Fig. 2.20. Difficulties were found in earlier non-LTE studies of the He I λ10 830 Å line: the observed trends of W_λ as a function of $T_{\rm eff}$ were not reproduced by the models, which predicted either too strong absorption or strong emission. These problems were related to inaccurate photoionization cross-sections and the neglect of line blocking – they are reliably solved now.

Little is known about near-IR metal lines in OB-type stars and BA-SGs alike. Because of this, we initiated a pilot study on both kind of stars using the high-resolution near-IR spectrograph CRIRES (Käufl et al. 2004) on the ESO VLT. First results are encouraging, showing good agreement between analyses from the near-IR spectra and previous modelling in the optical for some ions, see Fig. 2.21. However, huge efforts are still required to identify a number of photospheric absorption and emission

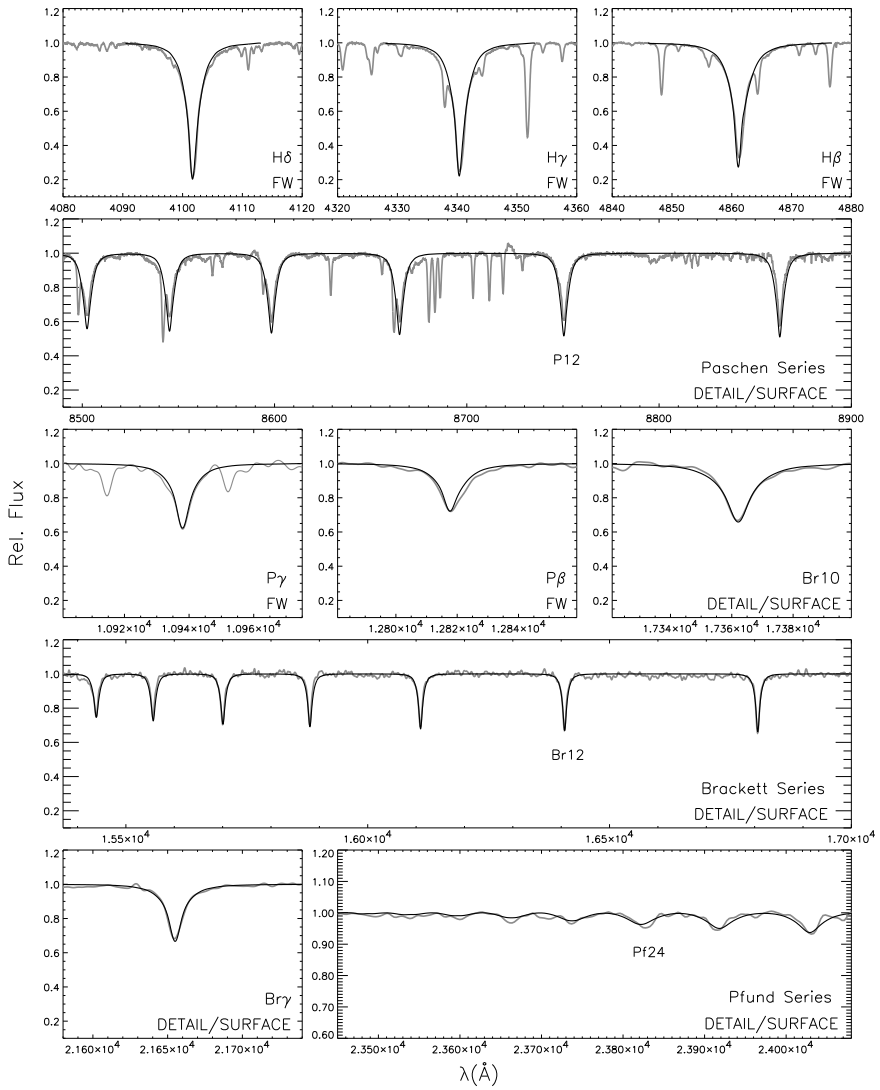

Figure 2.19: Modelling (black lines) of the hydrogen lines in the visual and the near-IR spectrum (grey) of the Galactic A-SG Deneb (A2 Ia). Overall, excellent agreement is achieved. The synthetic spectra are calculated with DETAIL/SURFACE (photospheric lines) or FASTWIND (FW, wind-affected lines), as indicated, for the same stellar parameters. Some lines, as Pβ and Hβ, are noticeably affected by the wind. From Schiller & Przybilla (2008).

lines and to extend/test model atoms for the use in the near-IR. Basic work has to be accomplished to determine all required atomic data for utilising near-IR transitions for quantitative studies in a comprehensive way, as the current status is meagre (see e.g. Johansson 2005).

The models and analysis methodology introduced previously are not restricted to the two object classes discussed here. We have already used these with great success for quantitative analyses of main sequence A-stars such as Vega (Przybilla 2002), chemically peculiar Bp stars (Przybilla et al. 2008c), subluminous B-stars (Przybilla et al. 2006b; Geier et al. 2007), extreme helium stars (Przybilla et al. 2005, 2006c), the Sun and solar-type stars (Przybilla & Butler 2004b; Mashonkina et al. 2007).

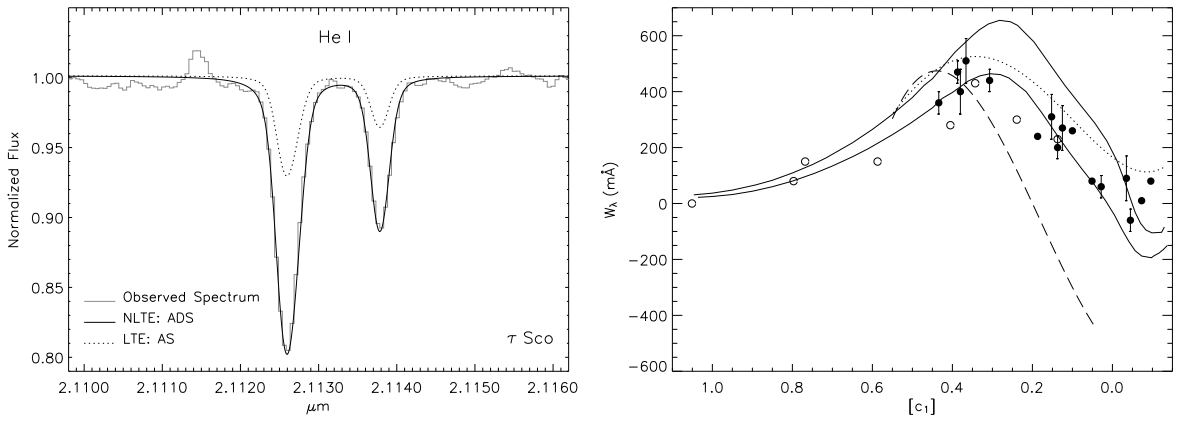

Figure 2.20: Modelling of helium lines in the near-IR. Left panel: non-LTE strengthening of the He I 2.11 μm lines in τ Sco. Stellar parameters as determined from the analysis in the optical have been adopted. From Nieva & Przybilla (2007). Right panel: comparison of observed equivalent widths for He I 10830 Å (Lennon & Dufton 1989: filled circles; Leone et al. 1995: open circles) with non-LTE model predictions (Auer & Mihalas 1973: dotted; Dufton & McKeith 1980: dashed; Przybilla 2005: full lines, for $\xi = 0$, lower, and 8 km s^{-1}, upper curve). The abscissa is the reddening-free $[c_1]$ index, a temperature indicator. From Przybilla (2005).

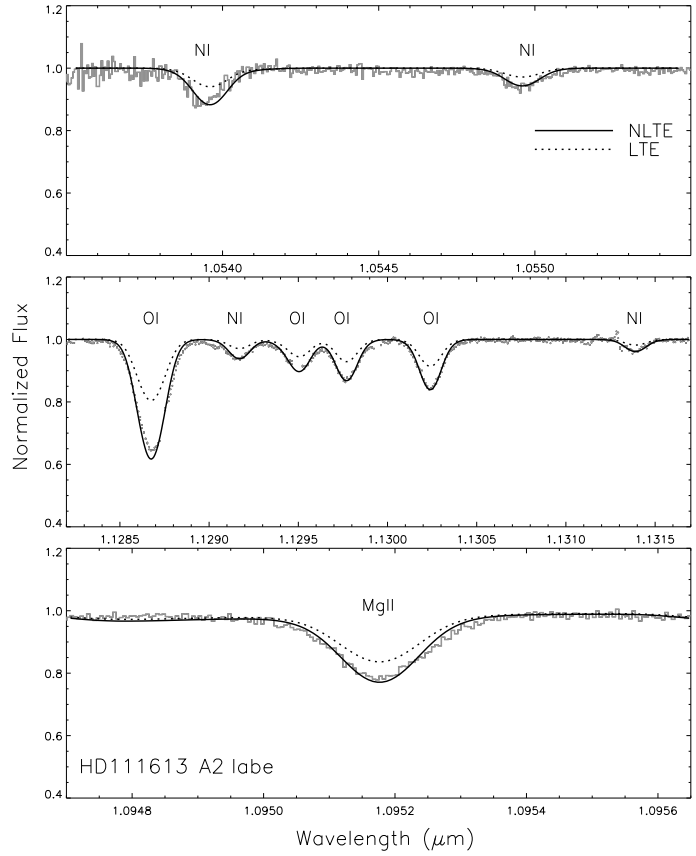

Figure 2.21: First results on high-resolution, high-S/N spectra of a bright Galactic A-type supergiant observed with CRIRES on the VLT. Stellar parameters and elemental abundances as determined from the analysis in the optical have been adopted for the modelling. Good agreement with observations is obtained in non-LTE, indicating reliability of the model atoms in these cases. Note that the telluric line correction (using HITRAN, Rothman et al. 2005) is not perfect for very strong telluric absorption – affected data points have therefore been omitted, like in the middle panel. From Przybilla et al. (2008f).

3 Observational Constraints on the Evolution of Massive Stars

A determination of accurate atmospheric parameters and elemental abundances for a larger sample of objects allows tight observational constraints on evolution models for massive stars to be derived. The most rewarding observational indicators for an empirical verification of the models are surface abundances of the light elements that participate in the main fusion cycle: carbon, nitrogen, helium, and, to a lesser degree, oxygen. These allow the otherwise inaccessible (magneto-)hydrodynamic mixing processes in the stellar interior to be traced. These processes redistribute angular momentum, transport burning products from the core to the surface and replenish hydrogen, thus extending lifetimes and increasing the stellar luminosity.

First results from an application of our analysis methodology to B-type dwarfs/giants and BA-type supergiants are summarised in Fig. 3.1. A comparison with evolution tracks is made. Most of the apparently slow-rotating B-stars show N/C ratios close to the pristine value of $\sim$0.3. A notable exception is τ Sco, which is a truly slow-rotating magnetic star (Donati et al. 2006). The situation is more complex with the BA-SGs. They all exhibit slow rotation because of their expanded envelopes, irrespective of the initial rotational velocity of their progenitors on the main sequence. It appears that the objects at masses below $\sim$15 $M_{\odot}$ show larger amounts of nuclear-processed material than those around $\sim$20 $M_{\odot}$. Larger N/C ratios are found again for the most massive objects of the sample. Note that the sample objects of $M \gtrsim 30\,M_{\odot}$ are located either in the Magellanic Clouds or in M31, i.e. they have a different metallicity than the Galactic stars.

Two important conclusions can already be drawn from this sample. Let us concentrate first on the objects more massive than $\sim$15 $M_{\odot}$. A general trend of increased mixing of nuclear-processed material with increasing stellar mass is found, in accordance with the predictions of evolution models (e.g. Heger & Langer 2000; Maeder & Meynet 2000). Moreover, the strongest mixing signature is found for the most metal-poor object, AzV 475 in the Small Magellanic Cloud, also in agreement with theory (e.g. Maeder & Meynet 2001). However, the mixing efficiency appears to be higher (by a factor $\sim$2) than predicted by current state-of-the-art evolution computations for rotating stars with mass-loss. Stellar evolution models accounting for the interplay of rotation and magnetic fields may resolve this discrepancy since they find a higher efficiency for chemical mixing (e.g. Maeder & Meynet 2005).

Larger N/C ratios at $M \lesssim 15\,M_{\odot}$ can be explained if the objects are on a blue loop, i.e. if they have already undergone the first dredge-up during a previous phase as a red supergiant, in addition to rotational mixing[4]. This interpretation is in contrast to earlier findings (e.g. Venn 1995b). Further support for the blue-loop scenario comes from lifetime considerations. Stellar evolution calculations

[4] Also in this case an increased mixing efficiency, by about a factor 2, would be required.

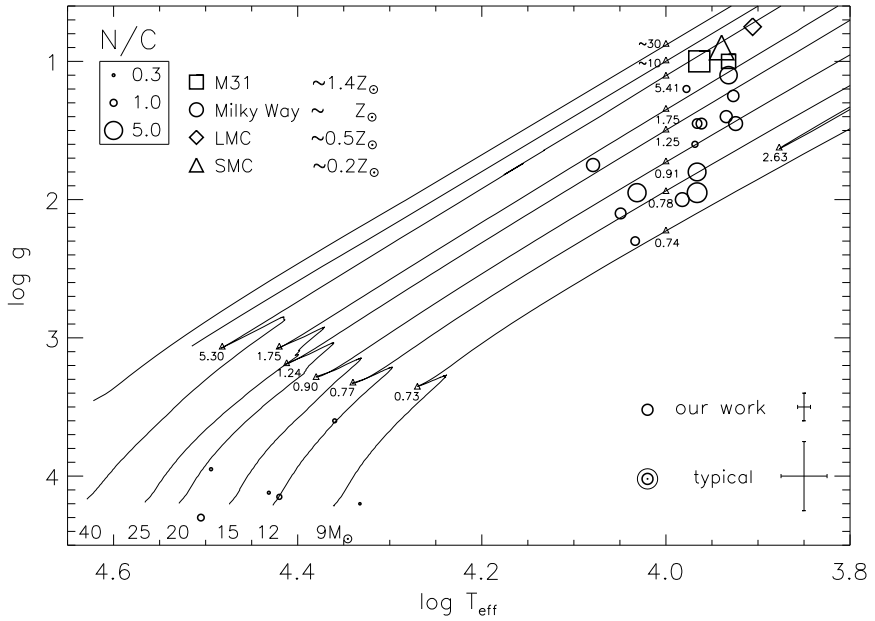

Figure 3.1: Observational constraints on massive star evolution. Displayed are results for the most sensitive indicator for mixing with nuclear-processed matter, N/C, in a homogeneously analysed sample of Galactic BA-type supergiants (circles) and their progenitors on the main sequence, OB dwarfs. The N/C ratios are encoded on a logarithmic scale, with some examples indicated. Error bars (1σ-statistical & systematic) from our work and those typical for previous work are also indicated. Stellar evolution tracks (Meynet & Maeder 2003) are displayed for rotating stars of metallicity $Z = 0.02$ (about solar $Z_\odot$ in older determinations like Anders & Grevesse (1989), full lines) – note that the observed metallicity for the Galactic sample is $Z \approx 0.014$. Starting with an initial N/C$\sim$0.3, theory predicts N/C$\sim$1 for BA-type supergiants evolving to the red, and N/C$\sim$2–3 after the first dredge-up. Since we find N/C values as high as $\gtrsim$6 the observed mixing efficiency is higher than predicted. Also, blue loops extend to hotter temperatures than predicted. A few results for objects in other Local Group galaxies are also shown. Summarising data from Przybilla et al. (2006a, 2008a,e), Firnstein (2006), Firnstein & Przybilla (2006), Nieva & Przybilla (2006, 2008), and from ongoing work.

indicate that supergiants spend a much longer time on a blue-loop (with central helium burning) than required for the crossing of the Hertzsprung-Russell diagram (HRD) from the blue to the red (the short phase of core contraction after central hydrogen burning has ceased). E.g., in the case of a rotating 9 $M_\odot$ model of Meynet & Maeder (2003) the difference is about a factor 15. It is well-established that blue loops are required to explain the Cepheid variables, but their extent in the HRD – in particular the upper limits in temperature and stellar mass – are essentially unknown. The blue-loop phase is highly sensitive to the details of the stellar evolution calculations ('... is a sort of magnifying glass, revealing relentlessly the faults of calculations of earlier phases.', Kippenhahn & Weigert 1990).

Consequently, a systematic and careful study of a larger sample of massive stars could provide the tight observational constraints required for a thorough verification and refinement of the stellar evolution models. More such precision analyses of stars covering the relevant part of the HRD are under way.

4 Observational Constraints on Galactochemical Evolution

Abundances of the heavier elements, from oxygen on, are unaffected by mixing in the course of stellar evolution in OB-type dwarfs/giants and BA-type supergiants. Also, chemical peculiarities are uncommon, as gravitational settling and/or radiative levitation apparently becomes effective only in stars of spectral types later than about B2 on the main sequence (e.g. Smith 1996). As a consequence, massive stars can be used as tracers of pristine abundances for the variety of elements detectable in their spectra.

The results of the abundance analysis for the B-star and BA-type supergiant sample are discussed next, with particular emphasis on the context of Galactochemical evolution. Note that while our B-star sample is located in the solar neighbourhood, the distribution of the BA-SGs is extended, out to distances of $\sim$3 kpc. As a result, the B-stars should be almost unaffected by a Galactic abundance gradient, whereas some effects may be present for the BA-type supergiants. This has to be kept in mind in the following discussion.

The status of previous non-LTE abundance studies of early B-type stars in the solar neighbourhood is illustrated in Fig. 4.1 (older LTE work is excluded). A wide range of abundance values is found for most elements, typically spanning $\sim$1 dex in total (for comparison, such a range is bridged by the cumulative effect of $\sim$13 Gyrs of Galactochemical evolution, see e.g. Fig. 2 of Chiappini 2003). Moreover, the abundance distributions peak in most cases at sub-solar values, in particular when referring to the solar composition of Grevesse & Sauval (1998). Exceptions are He, where most previous studies find values on average larger than solar, and Ne, which is about solar (Grevesse & Sauval 1998) as derived in the two very recent studies by Cunha et al. (2006) and Morel & Butler (2008). Several of these older B-star studies were combined by Snow & Witt (1996) and Sofia & Meyer (2001) to derive a reference composition, inevitably resulting in sub-solar average values and a large rms scatter (see Table 4.1). The former discrepancy has since been largely removed from a re-evaluation of solar abundances (Asplund et al. 2005). However, the status quo in terms of Galactochemical evolution can only be understood by invoking and fine-tuning extra processes such as infall/outflow of material and local retention of supernova products by large amounts.

On the other hand, our sample of early B-stars implies a *high degree of homogeneity* for present-day elemental abundances in the solar neighbourhood, with a scatter of $\sim$10%, and absolute values of about solar (Przybilla et al. 2008e). The only exception is nitrogen, which is most sensitive to mixing of the atmospheric layers with CN-processed material. In this case the pristine nitrogen abundance may be indicated by the 3 objects with the lowest value, implying a pristine N/C ratio of 0.31 ± 0.05 (by mass; error bar adjusted to reflect additional uncertainties). Note that mixing with nuclear-processed material will also affect the carbon abundances (oxygen and neon are expected to remain essentially unaffected until very late phases of stellar evolution). However, as the initial carbon abundance is much larger

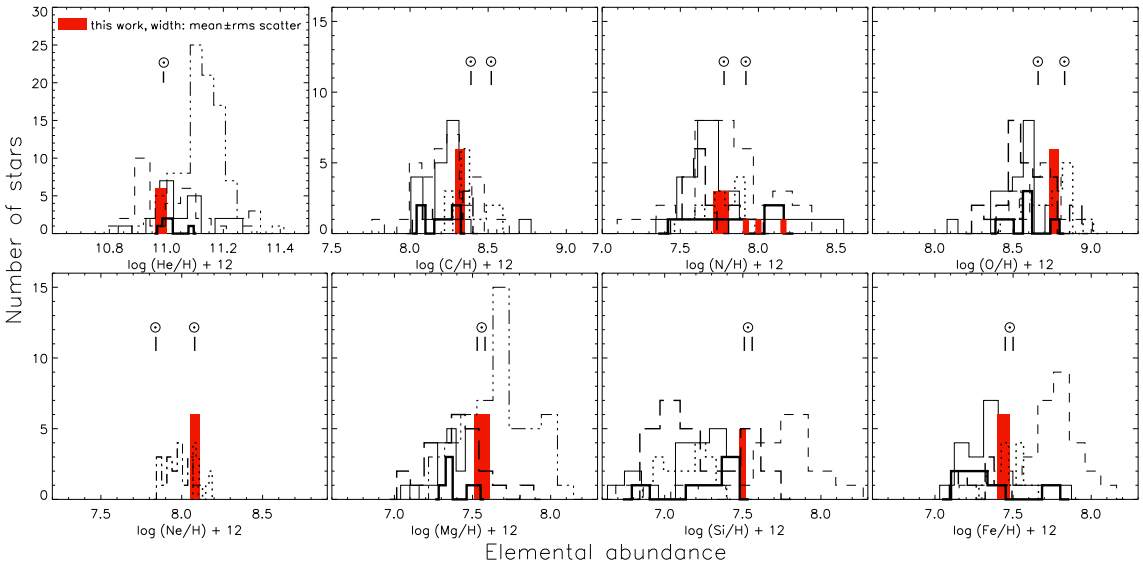

Figure 4.1: Comparison of chemical abundance studies (non-LTE) of B-type stars in the solar neighbourhood. Red bars: present work; full line and thick full line (for the same stars as in our work): Kilian (1992, 1994); dotted: Cunha & Lambert (1994), Cunha et al. (2006) for Ne; short-dashed: Gies & Lambert (1992), excluding bright giants and supergiants; long-dashed: Daflon et al. (1999, 2001a,b, 2003); dot-dashed: Morel & Butler (2008); triple-dot-dashed: Lyubimkov et al. (2004, 2005). Bin width is $\sigma/2$ of the individual studies. Iron abundances were derived assuming LTE in all previous work. Solar abundances are also indicated ($\odot$, Grevesse & Sauval 1998; Asplund et al. 2005: lower values). See text for details. From Przybilla et al. (2008e).

than the nitrogen abundance, little depletion is needed to produce a noticeable effect in nitrogen. Stellar evolution models (Meynet & Maeder 2003) predict depletion by up to $\sim$0.05 dex for stars of average rotation ($\sim$220 km s^{-1} on the main sequence) similar to our sample objects. Accounting for small corrections in the stars with N-enrichment, a pristine value of $\log \mathrm{C/H} + 12 = 8.35 \pm 0.05$ is indicated (Nieva & Przybilla 2008).

We regard our sample as representative for the early B-star population in the solar neighbourhood. The stars cover the relevant portion of the H-burning phase of the objects in the HRD in terms of $T_{\rm eff}$ and $\log g$ (see Fig. 3.1). They also sample one hemisphere of the solar neighbourhood (see Fig. 1 in Przybilla et al. 2008e), half of them located in OB associations and the other half in the field. All 6 stars were analysed by Kilian (1992, 1994), which we regard as one of the most accurate previous studies in terms of stellar parameter and abundance determination. Kilian's values for the 6 stars typically span the entire abundance range in her sample of 21 stars (see Fig. 4.1). We therefore also find a chance selection of stars with similar chemical composition for our sample unlikely. This is supported further by 6 BA-type supergiants in the solar neighbourhood (our 'control sample') – oxygen and magnesium abundances of these stars ($\log \mathrm{O/H} + 12 = 8.80 \pm 0.02$ and $\log \mathrm{Mg/H} + 12 = 7.55 \pm 0.07$) closely match those from the B-stars. The wide abundance ranges found in previous work reflect the lower accuracy of the analyses, while shifts of the abundance distributions relative to each other reflect systematics, with different temperature scales being the most important among these.

The finding of chemical homogeneity for our sample is in excellent accordance with results from the analysis of the ISM gas-phase in the solar neighbourhood (Sofia 2004, and references therein) and with theory regarding the efficiency of hydrodynamic mixing in the ISM (Edmunds 1975; Roy

Table 4.1: Chemical composition of different object classes in the solar neighbourhood and of the Sun

	cosmic standard	Orion		Young	ISM	ISM	
Elem.	B stars – this work	gas+dust[b]	B stars[c]	F&G stars[c]	gas	dust[d]	Sun[e/f]
He	10.98±0.02/ …[a]	10.988±0.003	…	…	…	…	10.99±0.02
C	8.35±0.05/224±27	8.52±0.02	8.28±0.17	8.55±0.10	8.15±0.06[g]	83±34	8.52±0.06/8.39±0.05
N	7.76±0.05/ 58±7	7.73±0.09	7.81±0.21	…	7.79±0.03[h]	…	7.92±0.06/7.78±0.06
O	8.76±0.03/575±41	8.73±0.03	8.54±0.16	8.65±0.15	8.59±0.01[i]	186±42	8.83±0.06/8.66±0.05
Ne	8.08±0.03/ 120±9	8.05±0.07	…	…	…	…	8.08±0.06/7.84±0.06
Mg	7.56±0.05/ 36±4	…	7.36±0.13	7.63±0.17	6.17±0.02[j]	34.8±4.4	7.58±0.05/7.53±0.09
Si	7.50±0.02/ 32±1	…	7.27±0.20	7.60±0.14	6.35±0.05[j]	29.6±2.2	7.55±0.05/7.51±0.04
Fe	7.44±0.04/ 28±3	…	7.45±0.26	7.45±0.12	5.41±0.04[j]	27.3±2.7	7.50±0.05/7.45±0.05

[a] in units of $\log(\mathrm{El/H})+12$ / atoms per 10^6 H nuclei; [b] Esteban et al. (2004); [c] Sofia & Meyer (2001); [d] difference between the cosmic standard and ISM gas-phase abundances, in units of atoms per 10^6 H nuclei; [e/f] Grevesse & Sauval (1998)/Asplund et al. (2005), photospheric values; [g] Sofia (2004); [h] Meyer et al. (1997), corrected according to Jensen et al. (2007); [i] Cartledge et al. (2004); [j] Cartledge et al. (2006)

& Kunth 1995). Excellent agreement is also obtained with elemental abundances in the Orion nebula (Esteban et al. 2004, see Table 4.1), with the exception of carbon, which may be a consequence of the atomic data used in the Orion analysis (see Nieva & Przybilla (2008) for the stellar case) plus overestimated dust corrections.

We propose to identify the abundances derived from the B-star sample (Table 4.1) with a *cosmic abundance standard*, the reference composition of cosmic matter in the solar neighbourhood at present day. Combining our B-star abundances with data for S, Cl and Ar from the analysis of the Orion nebula (Esteban et al. 2004) and solar meteoritic values for other abundant refractory elements (with $\log(\mathrm{El/H})+12 \gtrsim 5$, Asplund et al. 2005) allows mass fractions for hydrogen, helium and the metals to be derived. Accordingly, values of $X=0.715$, $Y=0.271$, $Z=0.014$ and $Z/X=0.020$ characterise the present-day cosmic matter in the solar neighbourhood (to be compared to protosolar values $X_0=0.7133$, $Y_0=0.2735$, $Z_0=0.0132$, Grevesse et al. 2007; $X_0=0.7110$, $Y_0=0.2741$, $Z_0=0.0149$, Lodders 2003).

These combined abundances are our recommended values for a wide range of applications requiring an accurate knowledge of the chemical composition at present (e.g. for opacity calculations), examples being models of star/planet formation or stellar evolution (in particular of short-lived massive stars), or for the empirical calibration of Galactochemical evolution models. In particular, our values for oxygen and neon introduce a new aspect to the ongoing discussion about discrepancies of helioseismic constraints and the solar interior model based on the recently revised solar abundances of Asplund et al. (2005), as discussed e.g. by Bahcall et al. (2005) and Basu & Antia (2008).

In a first application we have used the B-star abundance standard as proxy for a high-precision determination of the primary constituents of the ISM dust-phase composition (Przybilla et al. 2008e, cf. Table 4.1). The amount of material incorporated into dust grains is determined by the difference between our B-star abundances and the ISM gas-phase abundances. A composition poor in carbon but rich in oxygen and refractory elements is indicated. Tight constraints are put on dust models for the first time as a consequence of the small uncertainties in both components (in contrast to earlier work using averages over B- and young F- & G-star samples from the literature, see also Table 4.1).

The findings from the B-star sample are supported by the results from the BA-type supergiants, see Fig. 4.2 for a comparison. Despite lacking the high degree of homogeneity of the B-stars (a result of the larger volume sampled), the BA-SGs show a much smaller range in abundance than previous studies. The average abundances for O and Mg are in excellent agreement with the values from the B-stars, in particular from the 6 objects in the solar neighbourhood (the 'control sample'), but also from those at

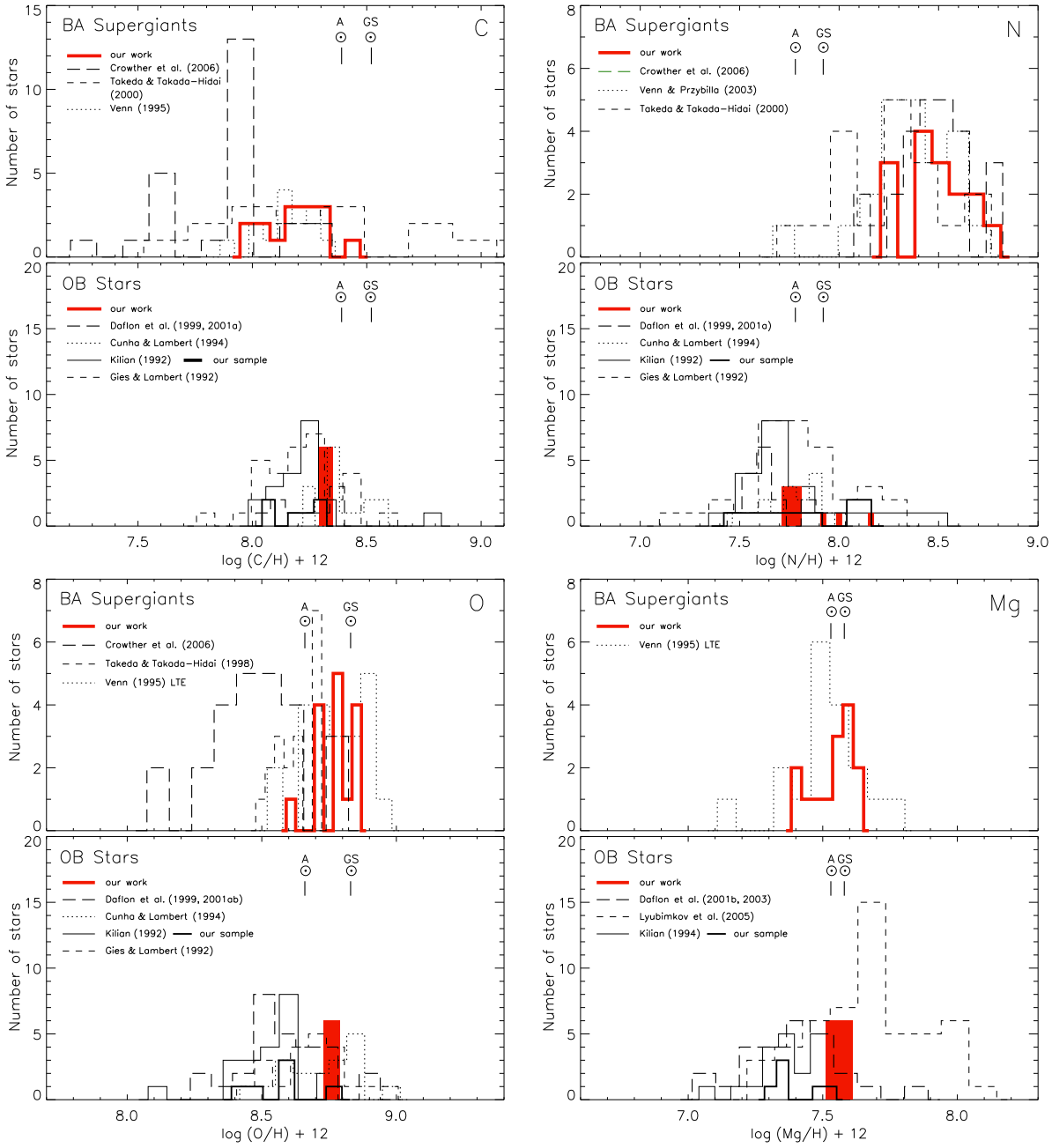

Figure 4.2: Comparison of B-star (in the solar neighbourhood) and BA-SG (out to ∼2.5 kpc distance) abundances for C, N, O and Mg as obtained in our work and from the literature, in analogy to Fig. 4.1. Carbon and nitrogen show clear indications of mixing with nuclear-processed matter in the BA-SGs. On the other hand, good agreement is found for oxygen and magnesium, both unaffected by stellar evolution. The BA-SG sample shows a slightly wider spread because a larger volume was investigated such that an influence of the Galactic abundance gradient/intermediate-scale inhomogeneities can become apparent. Summarising results from Firnstein (2006), Nieva & Przybilla (2008), Przybilla et al. (2006a, 2008e).

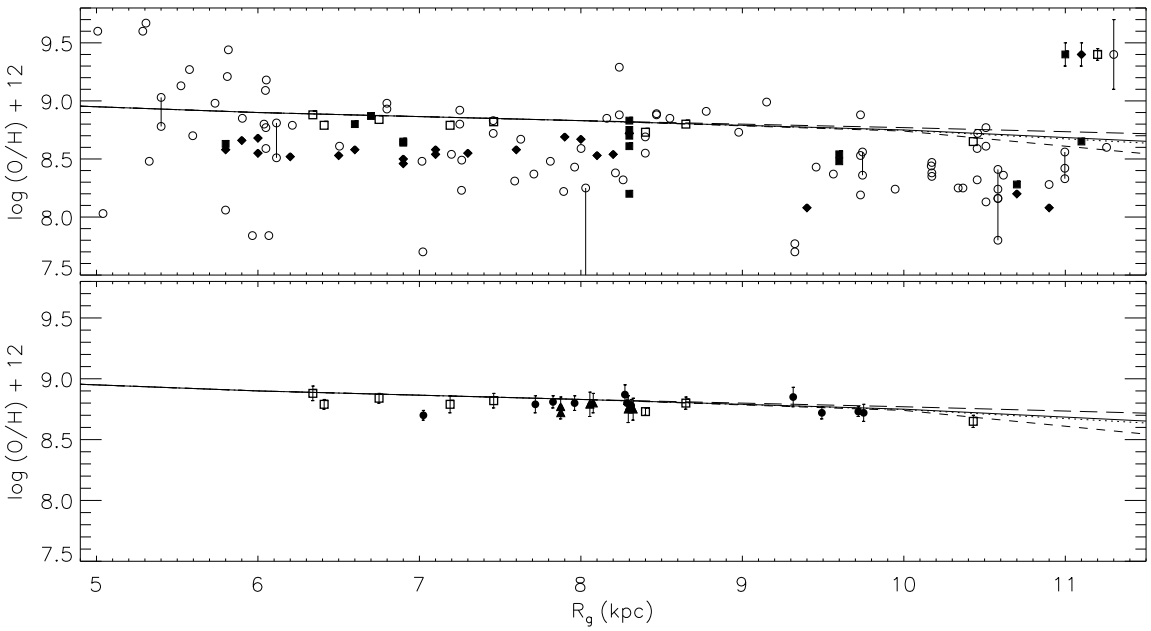

Figure 4.3: The Galactic oxygen abundance gradient. Upper panel: detail of Fig. 1.1. Lower panel: first results from our work on BA-type supergiants (dots) and B-stars (triangles). Individual error bars are indicated (1-σ statistical uncertainties), lines mark model predictions of Chiappini et al. (2001), see Fig. 1.1. *A clear trend is found and the scatter in abundance is dramatically reduced when typical systematic errors are eliminated*. From the stars alone (baseline of $\sim$3 kpc) a flat Galactic oxygen abundance gradient of -0.007 ± 0.016 dex kpc^{-1} is indicated. Excellent agreement with the work of Esteban et al. (2005) on H II regions (boxes) is found after applying a correction of $+0.08$ dex – as adopted by Esteban et al. (2004) for Orion – to account for depletion on dust grains in the nebulae. Using the combined sample of stars and H II regions the gradient becomes -0.028 ± 0.009 dex kpc^{-1}, extending the baseline to $\sim$4.5 kpc. Typically, a steeper gradient of about -0.07 dex kpc^{-1} is discussed in the literature, see Gummersbach et al. (1998) for an overview. Data from Przybilla et al. (2006a, 2008e) and Firnstein (2006).

larger distances. Carbon is depleted and nitrogen enriched as a consequence of the evolved state of the supergiants. The upper limit of carbon abundances in the BA-SGs is consistent with the pristine value derived from the B-stars, meeting a boundary condition imposed by mixing.

Consistency is achieved from two classes of indicators, which show completely different spectra (BA-SG spectra are dominated by neutral and single-ionized species, B-type stars by higher ionization stages). These first results imply that a re-interpretation of studies of massive, early-type stars in the context of Galactochemical evolution is required. It appears that previous findings of chemical inhomogeneity (Figs. 1.1 & 4.2) were a result of the limited accuracy of the models and the analysis methodology (e.g. photometric temperatures) used. A much higher degree of homogeneity is indicated from our work, which needs verification for the solar neighbourhood from a larger sample of objects. The work also requires an extension to other regions of the Milky Way to study star clusters and OB associations.

Now we have the tools at hand to determine abundances to the precision necessary to derive unbiased elemental abundance gradients in the Milky Way. For the most part, relatively steep abundance gradients (of about -0.07 dex kpc^{-1}, see e.g. Fig. 1.1 and Fig. 4.3, upper panel) are discussed in the literature, see Gummersbach et al. (1998) for an overview. And, the abundance indicators usually show

a large scatter around the mean trend. On the other hand, our first results on the Galactic abundance gradient imply a flat gradient and little scatter, see Fig. 4.3 (lower panel) for an example of the dramatic improvements that can be expected. Note that dust depletion introduces a source of systematic uncertainty to abundances determinations from H II regions for some elements, but it is irrelevant in the stellar case.

Such a flat abundance gradient is in accordance with the identification of the Milky Way as a barred spiral (e.g. López-Corredoira et al. 2007). Barred spiral galaxies usually show shallow abundance gradients (e.g. Zaritsky et al. 1994), which may be attributed to homogenisation due to large-scale radial gas flows induced by the bar (e.g. Roberts et al. 1979). Assuming the flat gradient to be confirmed by analysis of a larger sample of objects covering the entire extent of the Galactic disk this could remove the need to accept the Milky Way as an exception to the observed trend for barred spirals. An extension of the analyses, also with regard to the elements considered, will provide tight observational constraints on Galactochemical evolution models and may guide future improvements of the modelling.

5 Hypervelocity Stars

Observational studies of the stellar dynamics in the central arcsecond of our Galaxy over the past $\sim$15 years have provided strong evidence for the presence of a supermassive black hole (SMBH) in the Galactic centre (GC), coinciding with the radio source Sgr A* (e.g. Schödel et al. 2002; Ghez et al. 2005). Three-body interactions of binary stars with the SMBH will inevitably lead to the ejection of stars with velocities exceeding the escape velocity of our Galaxy[5] (Hills 1988; Yu & Tremaine 2003), so-called *hyper-velocity stars* (HVSs). The GC is therefore the *suspected* place of origin of the HVSs. Brown et al. (2006a) estimated that the Galactic halo holds $\sim$2000 HVSs in a sphere of 120 kpc radius. If the GC hosts a tight binary of a SMBH and an intermediate-mass black hole (IMBH), the formation rate of HVSs is ten times larger (Yu & Tremaine 2003). The detection of a binary HVS would be the smoking gun for a massive binary black hole, as a single SMBH cannot eject a binary star.

Hypervelocity stars are not only fascinating objects in their own right, but they may also be indicators of the properties of the SMBH in the GC and the surrounding stellar population. Moreover, HVSs are also regarded as valuable probes for the shape of the Galactic dark matter halo because of the unique kinematic properties of stars expelled from the GC (Gnedin et al. 2005; Yu & Madau 2007). Because of the importance of HVSs to astrophysics it is mandatory to study HVSs in as much detail as possible.

The first HVSs have only recently been discovered serendipitously (Brown et al. 2005; Hirsch et al. 2005; Edelmann et al. 2005; Heber et al. 2008). A total of 17 faint blue stars at high Galactic latitude have been identified as HVSs so far after a systematic search (see Brown et al. 2006a,b, 2007, 2008). Supposedly none is a binary star, as they all show constant radial velocities to within the measuring precision. So far, the sample is too small to make comprehensive conclusions on the HVS population in general, in particular as little more information than photometry, radial velocities and a coarse spectral classification is available for most objects. The reason for this is the faintness of most HVSs ($V \gtrsim 18$ mag), preventing them from being studied at high spectral resolution with telescopes of the 8–10m-class. This will become feasible only with future extremely large telescopes.

However, a few HVSs are bright enough to be studied in detail. The aim is to characterise the stars (fundamental stellar and atmospheric parameters, elemental abundances) as thoroughly as possible in order to allow a *reliable* determination of (spectroscopic) distances, lifetimes and the place of origin, to test Hills' scenario for HVS ejection. In particular, high precision is required in the abundance determination, as the expected chemical signature – α-enhancement for stars born near the GC – differs from the solar composition (as typical for a disk star) by only a factor $\sim$2. Application of our improved non-LTE modelling and analysis techniques provides the necessary precision, as discussed in Sect. 2. An example of the excellent quality of our final model fits to observation is shown in Fig. 5.1, results are summarised in Table 5.1. We thus pioneer the field of *quantitative spectroscopy of hyper-velocity stars*.

[5]The partner of the original binary will end up in a tight orbit around the SMBH, like the members of the S star population (Löckmann et al. 2008).

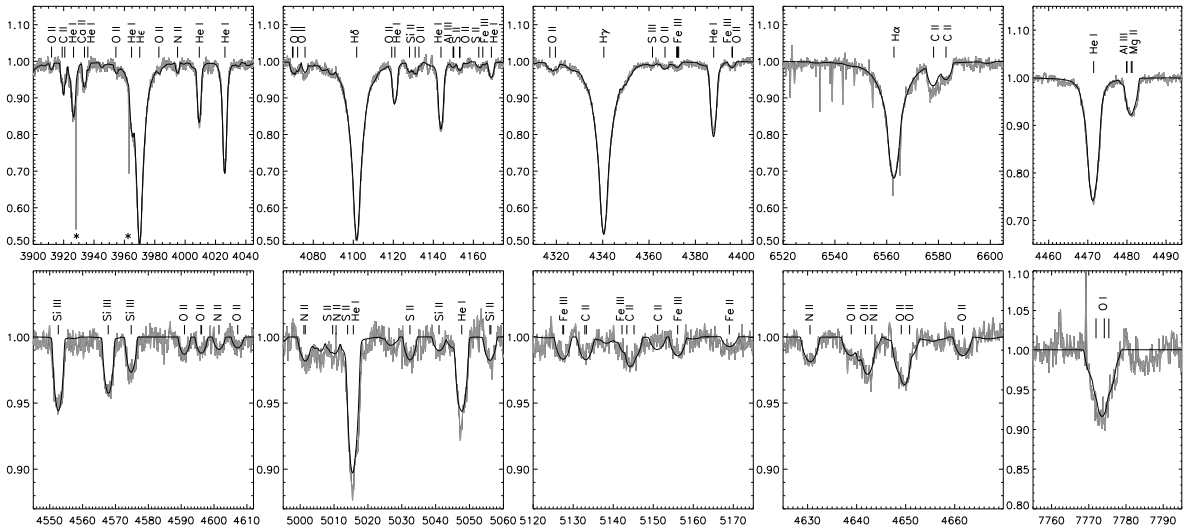

Figure 5.1: Comparison of spectrum synthesis for HD 271791 (full line) with observation (grey). The upper panels illustrate the excellent fit of Balmer and He I lines. The ionization equilibria of Si II/III, O I/II, S II/III and Fe II/III are perfectly matched (lower panel, plus S III λ4361 Å above). A selection of lines from most ions detected can be found in the panels. Note that all atmospheric features of the observed spectrum are simultaneously reproduced by the final model spectrum. Abscissa is wavelength (in Å), ordinate is normalised flux. Interstellar Ca II lines are marked by an asterisk. From Przybilla et al. (2008d).

Table 5.1: Properties of three hyper-velocity stars

	HE 0437−5439	HD 271791	HVS 7
Type	early B-dwarf	early B-giant	Bp star
V (mag)	16.36	12.26	17.80
$T_{\rm eff}$ (K)	23 000±1000	18 000±500	12 000±500
$\log g$ (cgs)	3.95±0.10	3.10±0.10	3.80±0.10
$v \sin i$ (km s^{-1})	55±2	124±2	55±2
$v_{\rm rad}$ (km s^{-1})	+723±3	+441±1	+529±2
$M/M_\odot$	9.1±0.8	11±1	3.7±0.2
$\tau_{\rm evol}$ (Myr)	18±3	25±5	150±10
d (kpc)	61±9	21±4	59±6

HE 0437−5439 (HVS 3). HE 0437−5439 was discovered by Edelmann et al. (2005) to be a hyper-velocity star located at a distance of $d = 61$ kpc. A heliocentric velocity $v_{\rm rad}$ of +723 km s^{-1} (see Table 5.1) is found for this early B-type dwarf, corresponding to a Galactic rest-frame velocity of at least 563 km s^{-1} (this value increases for non-zero proper motion). From a kinematic analysis Edelmann et al. (2005) concluded that this star originated in the Large Magellanic Cloud (LMC), because the time of flight from the Galactic Centre would exceed the age of the star ($\tau_{\rm evol}$, Table 5.1) by a factor of ∼3–4. A precise abundance determination may constrain this hypothesis further, as the baseline metallicity of the LMC (about half solar) differs significantly from the chemical signature of stars in the GC.

We analysed high resolution spectra of HE 0437−5439 obtained with UVES on the ESO VLT (Przybilla et al. 2008b). A comparison of the derived abundance pattern with the GC reference composition and our analysis results for two objects from the LMC and the solar neighbourhood is shown in Fig. 5.2.

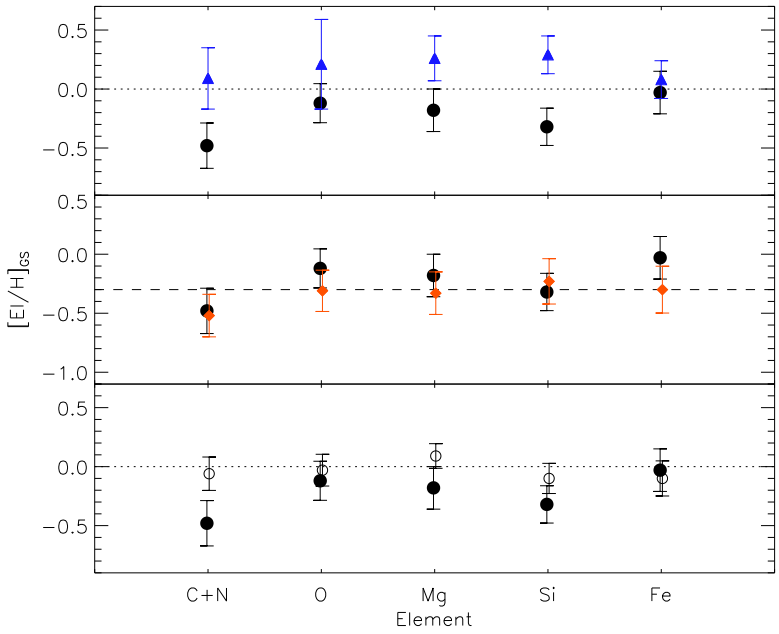

Figure 5.2: Comparison of metal abundances in HE 0437−5439 (dots) with a sample of stars close to the GC (triangles) in the upper panel, the LMC reference star NGC 2004-D15 (diamonds) in the middle panel, and the solar neighbourhood reference star HR 3468 (circles) in the lower panel. Solar reference abundances are adopted from Grevesse & Sauval (1998). Error bars account for statistic and systematic uncertainties. The chemical signature of HE 0437−5439 does not show α-enhancement along with solar iron abundance, excluding a GC origin. The abundance pattern is compatible with ejection from the LMC, however an origin in the outskirts of the Galactic disk cannot be ruled out from the chemical signature alone. From Przybilla et al. (2008b).

The abundance pattern of HE 0437−5439 rules out the Galactic Centre as its place of birth. The LMC is the most likely place of origin. An ejection velocity of about 1000 km s^{-1} is implied for HE 0437−5439 in order for it to have reached its position from the LMC within its lifetime.

This requires an alternative ejection mechanism since no SMBH is known in the LMC. Dynamical ejection from a massive, dense star cluster (Leonard 1991) would be an option that needs further investigation. Candidate clusters within the LMC that are massive and dense enough, and that also have the right age, are NGC 2100, NGC 2004, NGC 1850 and NGC 1847. Alternatively, the disruption of a binary system by an IMBH of $\gtrsim 10^3\,M_\odot$ may be capable of accelerating one of the components to the observed high velocity (Gualandris & Portegies Zwart 2007). Again, dense clusters like NGC 2100 or NGC 2004 are suggested to harbour such a – so far unknown – IMBH (Gualandris & Portegies Zwart 2007). A measurement of the proper motion of HE 0437−5439 is required to trace its orbit for an unambiguous identification of its place of origin.

SDSS J113312.12+010824.9 (HVS 7). HVS 7 is a late B-type HVS discovered by Brown et al. (2006b), which may be an intermediate-mass main-sequence object or alternatively a low-mass horizontal branch star. Located at a distance of 59 kpc (in the main-sequence case) the star shows a Galactic rest-frame velocity of at least 421 km s^{-1}.

We analysed high-resolution spectra of HVS 7 obtained with UVES on the ESO VLT (Przybilla et al. 2008c). The star has a very low helium content of ∼1/100 solar. It is underabundant in the light

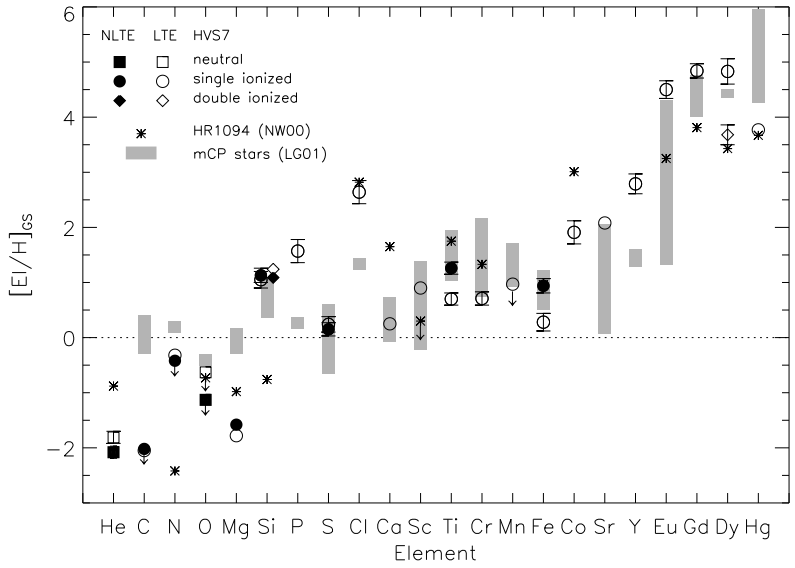

Figure 5.3: Abundance pattern of HVS 7, relative to solar values (Grevesse & Sauval 1998), compared with magnetic CP stars. Symbols are identified in the legend. The error bars represent statistical 1σ-uncertainties from the line-to-line scatter. Realistic errors, accounting for systematic effects (e.g. if a magnetic field were present), are expected to be larger. Upper limits are indicated by arrows. Asterisks mark abundances for the Cl-Co-rich B9p star HR 1094 (Nielsen & Wahlgren 2000) and grey bars abundance ranges observed in a sample of magnetic CP stars (López-García et al. 2001). From Przybilla et al. (2008c).

elements (C, N and O are below the detection limit) but shows strong enrichment of heavy elements (factors up to $\sim$10 000 times solar for rare-earth elements and mercury), see Fig. 5.3. The derived abundance pattern of HVS 7 is characteristic of the class of chemical peculiar magnetic B stars on the main sequence. However, the presence of chlorine and strong phosphorus and cobalt lines in the spectrum of HVS 7 is unusual even for CP stars. The chemical composition and high projected rotation velocity $v \sin i = 55\,\mathrm{km\,s^{-1}}$ make it unlikly that HVS 7 is a low-mass blue horizontal branch star.

Such a surface abundance pattern is caused by atomic diffusion (from the interplay of gravitational settling and radiative levitation) in a possibly magnetically stabilised[6], non-convective atmosphere. Hence all chemical information on the star's place of birth and its evolution has been washed out. High-precision astrometry for a determination of the proper motion is the only means to validate a GC origin for HVS 7.

HD 271791. HD 271791 is an early B-type HVS at a distance of about 20 kpc, discovered by Heber et al. (2008). This is the only HVS for which a proper motion has been measured with sufficient accuracy. Its Galactic rest-frame velocity is about $600\,\mathrm{km\,s^{-1}}$, hence the star is unbound. From its 3D-space motion Heber et al. (2008) concluded that this star has originated in the outer rim of the Galactic disk (see Fig. 4 in that paper), which excludes the SMBH slingshot mechanism. In order to find an alternative ejection scenario a detailed abundance analysis is required.

[6]We derive an upper limit of about 3 kG for the stellar magnetic field from identifying the observed microturbulence velocity with the extra broadening of metal lines due to the Zeeman effect (Kupka et al. 1996). This may put valuable constraints on magnetic fields in the GC if HVS 7 could be proven to be of GC origin and the field as being of fossil origin (note that the star S2 near the GC is also suggested to be magnetic, Martins et al. 2008).

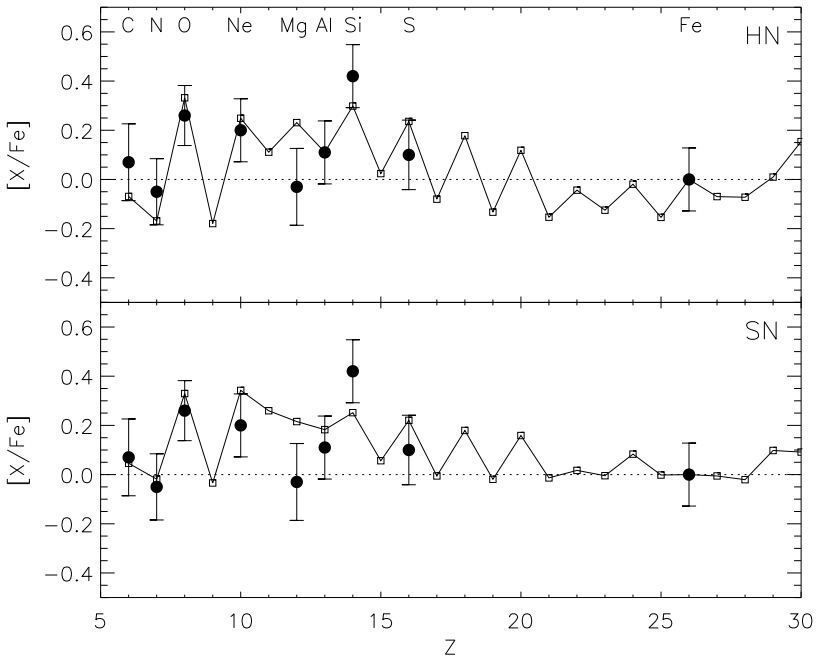

Figure 5.4: Elemental abundance pattern of HD 271791 (dots, relative to solar (Grevesse & Sauval 1998) as a function of atomic number Z, normalised to Fe) compared to hyper-/supernova yields of Nomoto et al. (2006). Error bars account for statistical and systematic uncertainties of 0.1 dex, summed in quadrature. See text for details. From Przybilla et al. (2008d).

We analysed high resolution spectra obtained with FEROS on the 2.2m Max-Planck-ESO telescope in La Silla (Przybilla et al. 2008d). Figure 5.1 shows a few examples of the excellent fit quality achieved with the final synthetic spectrum. The abundance pattern of HD 271791 is exceptional: sub-solar iron along with enhancement of the α-elements is found, making HD 271791 the first massive Population I star outside the GC (though at low [Fe/H]) to show such characteristics.

The low iron abundance is consistent with the birth place of the star indeed being located in the metal-poor outer rim of the Galactic disk. On the other hand, α-enhancement indicates capture of nucleosynthesis products from a core-collapse supernova (SN), as reported e.g. for the secondary in the low-mass X-ray binary Nova Scorpii 1994 (Israelian et al. 1999). This implies that HD 271791 is the surviving secondary of a massive binary system disrupted in a supernova explosion. No such run-away star (scenario of Blaauw 1961) has ever been found to exceed the Galactic escape velocity, hence HD 271791 is the first *hyper-runaway star*. Such a run-away scenario has therefore to be viewed as an alternative to the Hills mechanism for the acceleration of some HVSs with moderate velocities. The observed chemical composition of HD 271791 puts invaluable observational constraints on nucleosynthesis in a supernova from the core-collapse of a very massive star ($M_{\rm ZAMS} \gtrsim 55\,M_{\odot}$), which may be observed as a gamma-ray burst of the long-duration/soft-spectrum type.

A plausible evolutionary scenario for the binary system was developed (Przybilla et al. 2008d), consisting of a Wolf-Rayet primary (of WC type) and a main-sequence B-type secondary (HD 271791) in close orbit previous to the system's disruption. The final collapse of the WC star into a black hole (Heger et al. 2003) resulted in an ordinary type Ic SN or a more energetic hypernova (HN). Nucleosynthesis products were accreted from the expanding SN-shell onto the secondary (Fryxell & Arnett 1981). Also

interaction with fall-back material from the explosion could have been significant (Podsiadlowski et al. 2002). Later, the accreted material was partially mixed with unpolluted matter from the secondary's deeper layers (and possibly with CN-processed material from its core).

A comparison of the model predictions (using HN-/SN-yields of Nomoto et al. 2006) with observation is shown in Fig. 5.4. Overall, reasonable agreement between the model predictions and observation is obtained, except that too large a magnesium and too low a silicon abundance are predicted. However, this is likely an artifact of the use of integrated yields. More realistic is a latitudinal dependency of the ejecta composition in the likely case of an aspherical explosion (Maeda et al. 2008) and a stratified abundance distribution in the ejecta. Hydrodynamic instabilities at the trailing edge of the SN-shell will preferentially lead to an accretion of material from the inner shell on the secondary (Fryxell & Arnett 1981), which is rich in silicon and depleted in magnesium (e.g. Maeda et al. 2002). Tailored nucleosynthesis calculations for this particular case and a detailed hydrodynamical simulation of the SN-shell–secondary interaction have since been initiated.

Conclusions. The precision analysis of high-resolution spectra of hyper-velocity stars has uncovered three highly interesting objects, though none could be unambiguously related to a GC origin. Contrary to expectation, one HVS was shown to originate in the outskirts of the Milky Way and another highly likely to have come from the LMC, providing evidence that alternative scenarios to Hills' slingshot mechanism are also in operation. It has already become clear, even at this early stage, that the field of hyper-velocity stars is much more complex than one may initially have thought.

6 Extragalactic Stellar Astronomy

Quantitative spectroscopy of massive, early-type stars is feasible also in nearby galaxies, because of the immense luminosity of OB-type stars and in particular BA-type supergiants. This opens up the possibility to study stellar evolution as a function of metallicity, one of the key quantities of the models, and of galactochemical evolution in different environments.

Local Group. Earlier versions of our model atoms were used by Korn et al. (2002, 2005) in an analysis of high-resolution spectra of unevolved B-stars in the Large Magellanic Cloud (LMC). Pristine present-day abundances of the light elements were obtained from stars for the first time. It was shown that the LMC is indeed nitrogen-poor, as indicated earlier by studies of H II regions (Garnett 1999). More work on OB-type dwarfs/giants is required to study both slow and fast rotators in order to derive comprehensive observational constraints on the evolution models near the main sequence. Here, the FLAMES survey of massive stars (Evans et al. 2005, 2007) provides a unique database for three galaxies: the Milky Way, the Large, and the Small Magellanic Cloud.

First results from an application of our analysis methodology to high-resolution spectra of selected A-type supergiants in the Magellanic Clouds and in M 31 are shown in Fig. 3.1, cf. also Venn & Przybilla (2003). An extension of the work to larger samples of supergiants in these and other galaxies of the Local Group will in particular allow the metallicity-dependent mixing efficiency of stellar evolution models (e.g. Maeder & Meynet 2001) to be verified.

A-type supergiants as tracers for galactochemical evolution were studied at high spectral resolution in several galaxies of the Local Group. These comprise first steps towards a determination of abundance gradients/patterns in spiral galaxies like M 31 (Venn et al. 2000) or in dwarf irregular (dIrr) galaxies like NGC 6822 (Venn et al. 2001). Gas-rich dIrr galaxies are of particular interest, as they are the closest analogues to the basic building blocks in hierarchical galaxy formation scenarios ('near-field cosmology'). Detailed information on abundances for various elements permits deeper insights in the nucleosynthesis histories of dIrr galaxies beyond the Magellanic Clouds to be obtained (Venn et al. 2003, and references therein). Progress in this branch of extragalactic stellar astronomy is slow, as high-resolution spectroscopy of supergiants at these distances is costly. Several hours of observing time on 8-10m-class telescopes are required per object.

Quantitative studies at intermediate spectral resolution allow only less-comprehensive information to be derived. However, they also have their advantages: large observational samples can be easily accessed using multi-object spectrographs, and fainter targets become observable (see e.g. Urbaneja et al. 2008), facilitating *quantitative spectroscopy of supergiants in galaxies beyond the Local Group*.

Beyond the Local Group. Observations of blue supergiant candidates in NGC 3621 (Fig. 6.1) at a distance of 6.6 Mpc pushed the capabilities of FORS1 and the ESO VLT to their limits. Spectra of 19 objects down to $V \approx 22$ mag were obtained in 10.7 hrs of integration time, confirming many

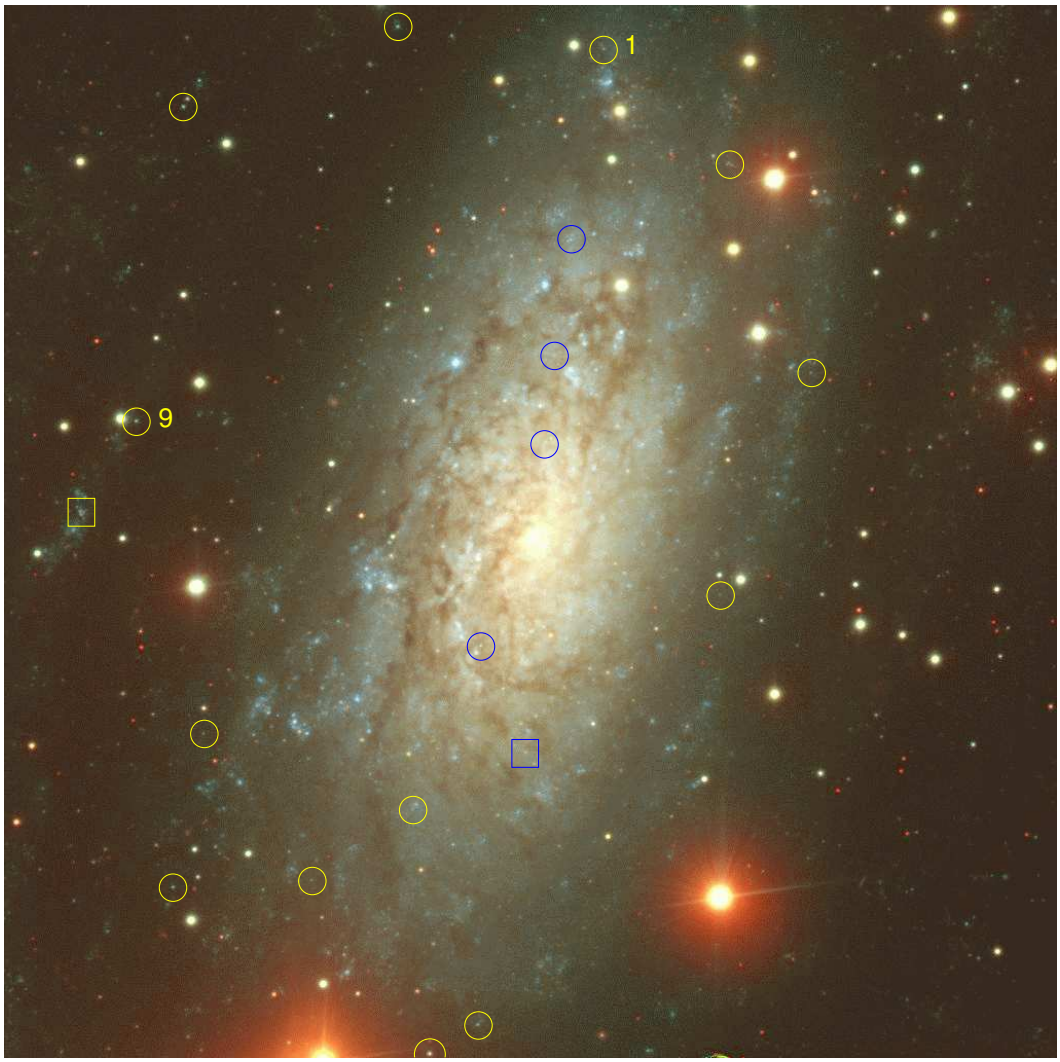

Figure 6.1: NGC 3621 at a distance of 6.6 Mpc. The positions of stars (circles) and H II regions (boxes) observed with FORS1 on the ESO VLT are marked on a colour image obtained by combining 5 min B, V and I-band frames taken with the same instrument in imaging mode. The field of view is approximately $7' \times 7'$. Different coloured markers are used for clarity only. From Bresolin et al. (2001).

as supergiants (Bresolin et al. 2001). Intermediate-resolution spectra can be quantitatively analysed once a reliable and comprehensive modelling is achieved (Fig. 2.17, see Przybilla et al. 2006a for thorough tests). However, medium-resolution spectroscopy implies a loss in detail and accuracy of the information that can be extracted from observation. We expect that metallicities can be determined to better than a factor $\sim$2, i.e. at an accuracy similar to that achieved in many published high-resolution studies. Our modelling is therefore *highly competitive* in extragalactic research.

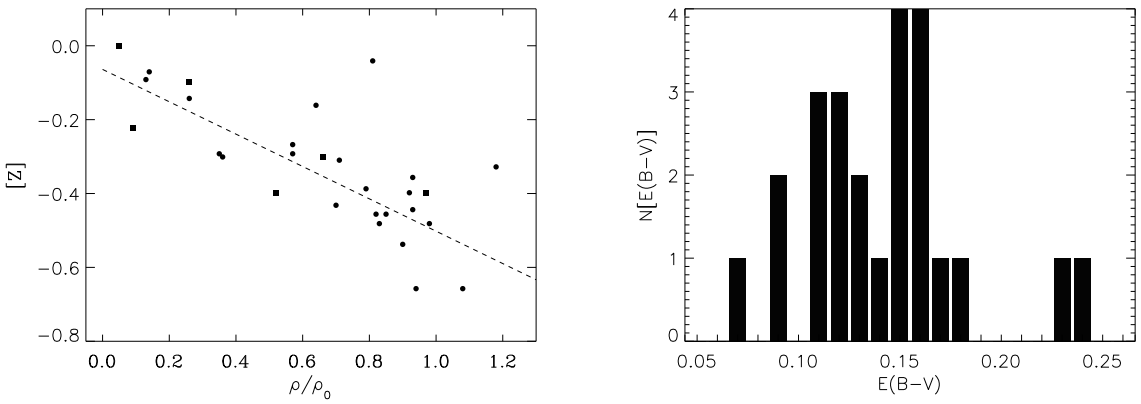

Figure 6.2: Left: Metallicity $[Z]$ as a function of angular galactocentric distance ρ/ρ_0 for A-SGs (filled circles) and early B-SGs (filled squares) in NGC 300. The dashed line represents the regression discussed in the text. Note that typical uncertainties in $[Z]$ are ± 0.2 dex. Right: Interstellar reddening $E(B-V)$ distribution of A-SG targets in NGC 300. From Kudritzki et al. (2008).

Such studies can be extended to larger samples of objects covering the entire extent of galaxies. This allows the results from the only indicators used so far, luminous H II nebulae, to be *verified* and *extended*. The most detailed study in this respect is on NGC 300, a spiral galaxy in the nearby Sculptor Group observed within the Araucaria project (Gieren et al. 2005). A total of 30 blue supergiants have so far been analysed (Bresolin et al. 2002; Urbaneja et al. 2005; Kudritzki et al. 2008), including 24 BA-type supergiants which were studied using modelling techniques developed by Przybilla et al. (2006a). A metallicity gradient of $-0.08\,\mathrm{dex\,kpc^{-1}}$ is derived for this Sc-type spiral, see Fig. 6.2.

Abundances from nebulae are in most cases derived by strong-line methods, i.e. empirical correlations between line ratios and abundance are used (like the R_{23}-index for oxygen), as the spectral features necessary for a direct analysis are often not observed because of their weakness. It turns out that absolute abundances and the abundance gradient from nebulae depend strongly on the calibration. Several of the most-widely used calibrations from the literature *fail* to achieve consistency with the stellar indicators: nebular abundances may be too large by up to a factor 2–3, and they may indicate an abundance gradient that is too steep (see Urbaneja et al. 2005 for details). Such discrepancies have also been found in other galaxies, from detailed analyses of H II regions (Kennicutt et al. 2003; Bresolin et al. 2004b). The presence of systematic bias in abundance studies based on photoionization models is also indicated (Stasińska 2005), in particular for metal-rich nebulae.

These examples indicate that the presently available observational constraints on galactochemical evolution (based on analyses of H II regions) may potentially be subject to serious systematic error, implying severe deficits in our preset-day understanding of galaxy evolution. Accurate analyses of extragalactic BA-type supergiants using our models have an enormous potential to improve on this, promising to provide thorough constraints for galactochemical evolution models.

Blue Supergiants & the Extragalactic Distance Scale. Blue supergiants allow not only for a determination of stellar metallicities, but also for the derivation of interstellar reddening and extinction in other galaxies. As an example, an averaged reddening of $\sim$0.12 mag is obtained for NGC 300, however with a large variation from 0.07 to 0.24 mag (see Fig. 6.2), which impacts Cepheid distances if not prop-

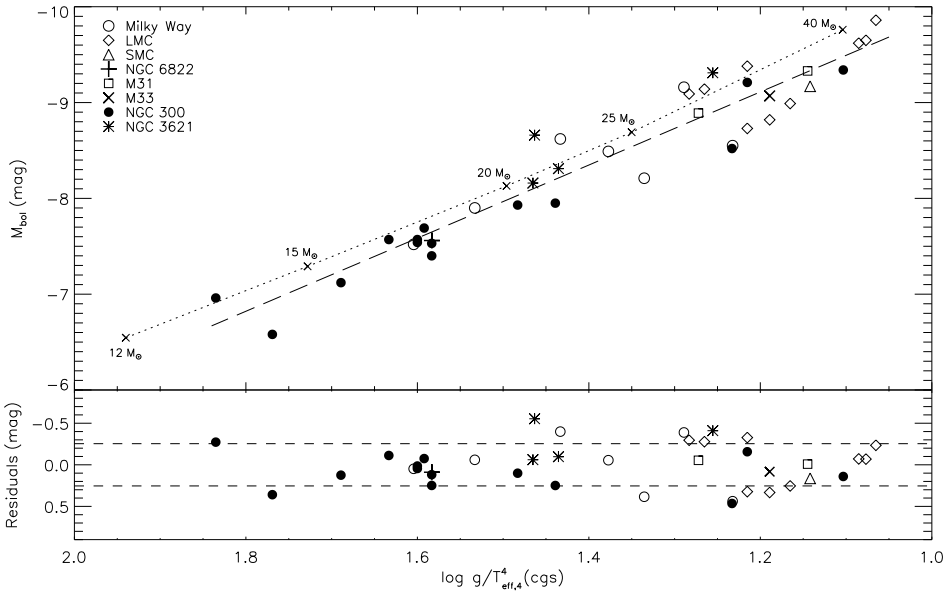

Figure 6.3: Absolute bolometric magnitude vs. logarithm of flux-weighted gravity of B8 to A4 supergiants in eight galaxies (see legend). The linear regression to the observational data is marked by a dashed line. The relationship obtained from stellar evolution models at solar metallicity and accounting for effects of rotation (Meynet & Maeder 2003) is also shown and labelled with the initial zero-age main-sequence masses of the corresponding models. Note that $T_{\rm eff}$ is used in units of 10^4 K. According to Kudritzki et al. (2003), with updates from Przybilla et al. (2006a, 2008a).

erly accounted for. Hence, blue supergiants can *indirectly* contribute to the work on the extragalactic distance scale. Systematic errors due to metallicity and extinction may be reduced in Cepheid studies. However, there is more to gain.

Precise stellar parameters of BA-type supergiants, as obtained from an application of our models, allow the flux-weighted gravity–luminosity relationship (FGLR, Kudritzki et al. 2003, 2008) to be exploited for *direct* distance determinations. The FGLR is a consequence of the fast evolution of BA-type supergiants from the blue to the red part of the HRD at roughly constant mass and luminosity (e.g. Maeder & Meynet 2000). Then, the stellar gravity and effective temperature are coupled through the relation $g/T_{\rm eff}^4 = \text{const}$. Assuming that the luminosity scales with stellar mass ($L \propto M^\alpha$, $\alpha \approx 3$), a relationship between absolute bolometric luminosity $M_{\rm bol}$ and flux-weighted gravity results, of the form

$$-M_{\rm bol} = a \log(g/T_{\rm eff}^4) + b\,, \tag{6.1}$$

see Kudritzki et al. (2008) for a detailed discussion. After an empirical calibration of the coefficients a and b this promises to become a highly robust distance determination technique[7] (Fig. 6.3). Many of the systematic uncertainties affecting the Cepheid distances can be avoided via this *spectroscopic* method. Quantitative spectroscopy of BA-type supergiants can therefore be expected to contribute in resolving the ongoing discussion on the value of the Hubble constant (Freedman et al. 2001; Sandage et al. 2006).

[7]Distances from the FGLR are not significantly affected by the intrinsic photometric variability of the blue supergiants (Bresolin et al. 2004a).

Bibliography

Albayrak, B. 2000, A&A, 364, 237

Allen, C. 1973, *Astrophysical Quantities*, 3rd ed. (Athlone Press, London)

Anders, E., Grevesse, N. 1989, Geochim. Cosmochim. Acta, 53, 197

Asplund, M., Grevesse, N., Sauval, A. J. 2005, in: T. G. Barnes III, F. N. Bash (eds.), *Cosmic Abundances as Records of Stellar Evolution and Nucleosynthesis* (ASP, San Francisco), 25

Auer, L. H., Mihalas, D. 1973, ApJS, 25, 433

Aufdenberg, J. P., Hauschildt, P. H., Baron, E., et al. 2002, ApJ, 570, 344

Bahcall, J. N., Basu, S., Pinsonneault, M., Serenelli, A. M. 2005, ApJ, 618, 1049

Basu, S., Antia, H. M. 2008, Phys. Rep., 457, 217

Becker, S. R. 1998, in: I. D. Howarth (ed.), *Boulder-Munich II: Properties of Hot, Luminous Stars* (ASP, San Francisco), 137

Becker, S. R., Butler, K. 1988, A&A, 201, 232

Bensby, T., Feltzing, S., Lundström, I. 2003, A&A, 410, 527

Blaauw, A. 1961, Bull. Astron. Inst. Netherlands, 15, 265

Bresolin, F., Kudritzki, R. P., Méndez, R. H., **Przybilla, N.** 2001, ApJ, 548, L159

Bresolin, F., Gieren, W., Kudritzki, R. P., Pietrzyński, G., **Przybilla, N.** 2002, ApJ, 567, 277

Bresolin, F., Pietrzyński, G., Gieren, W., Kudritzki, R. P., **Przybilla, N.**, Fouqué, P. 2004a, ApJ, 600, 182

Bresolin, F., Garnett, D. R., Kennicutt, R. C., Jr. 2004b, ApJ, 615, 228

Brown, W. R., Geller, M. J., Kenyon, S. J., Kurtz, M. J. 2005, ApJ, 622, L33

Brown, W. R., Geller, M. J., Kenyon, S. J., Kurtz, M. J. 2006a, 640, L35

Brown, W. R., Geller, M. J., Kenyon, S. J., Kurtz, M. J. 2006b, 647, 303

Brown, W. R., Geller, M. J., Kenyon, S. J., Kurtz, M. J., Bromley, B. C. 2007, ApJ, 671, 1708

Brown, W. R., Geller, M. J., Kenyon, S. J. 2008, ApJ, submitted (`arXiv:0808.2469 [astro-ph]`)

Burbidge, E. M., Burbidge, G. R., Fowler, W. A., Hoyle, F. 1957, Rev. Modern Phys., 29, 547

Butler, K., Giddings, J. R. 1985, Newsletter on Analysis of Astronomical Spectra, No. 9 (Univ. London)

Cameron, A. G. 1957, PASP, 69, 201

Cartledge, S. I. B., Lauroesch, J. T., Meyer, D. M., Sofia, U. J. 2004, ApJ, 613, 1037

Cartledge, S. I. B., Lauroesch, J. T., Meyer, D. M., Sofia, U. J. 2006, ApJ, 641, 327

Cayrel, R., Depagne, E., Spite, M., et al. 2004, A&A, 416, 1117

Cescutti, G., Matteucci, F., François, P., Chiappini, C. 2007, A&A, 462, 943

Chiappini, C., Matteucci, F., Romano, D. 2001, ApJ, 554, 1044

Chiappini, C., Romano, D., Matteucci, F. 2003, MNRAS, 339, 63

Cox, A. 2000, *Allen's Astrophysical Quantities* (Springer Verlag, Berlin)

Crowther, P. A., Lennon, D. J., Walborn, N. R. 2006, A&A, 446, 279

Cunha, K., Lambert, D. L. 1994, ApJ, 426, 170

Cunha, K., Hubeny, I., & Lanz, T. 2006, ApJ, 647, L143

Daflon, S., Cunha, K. 2004, ApJ, 617, 1115

Daflon, S., Cunha, K., Becker, S. R. 1999, ApJ, 522, 950

Daflon, S., Cunha, K., Becker, S. R., Smith, V. V. 2001a, ApJ, 552, 309

Daflon, S., Cunha, K., Butler, K., Smith, V. V. 2001b, ApJ, 563, 325

Daflon, S., Cunha, K., Smith, V. V., Butler, K. 2003, A&A, 399, 525

Dekker, H., D'Odorico, S., Kaufer, A., Delabre, B., Kotzlowski, H. 2000, Proc. SPIE, 4008, 534

Donati, J.-F., Howarth, I. D., Jardine, M. M., et al. 2006, MNRAS, 370, 629

Dufton, P. L., McKeith, C. D. 1980, A&A, 81, 8

Dufton, P. L., Brown, P. J. F., Lennon, D. J., Lynas-Gray, A. E. 1986, MNRAS, 222, 713

Edelmann, H., Napiwotzki, R., Heber, U., Christlieb, N., Reimers, D. 2005, ApJ, 634, L181

Edmunds, M. G. 1975, Ap&SS, 32, 483

Edvardsson, B., Andersen, J., Gustafsson, B., et al. 1993, A&A, 275, 101

Esteban, C., Peimbert, M., García-Rojas, J., et al. 2004, MNRAS, 355, 229

Esteban, C., García-Rojas, J., Peimbert, M., et al. 2005, ApJ, 618, L95

Evans, C. J., Smartt, S. J., Lee J. K., et al. (**Przybilla, N.**) 2005, A&A, 437, 467

Evans, C. J., Lennon, D. J., Smartt, S. J., Trundle, C. 2007, A&A, 464, 289

Faber, S. M., Phillips, A. C., Kibrick, R. I., et al. 2003, Proc. SPIE, 4841, 1657

Firnstein, M. 2006, Diploma Thesis, Univ. Erlangen-Nuremberg

Firnstein, M., **Przybilla, N.** 2006, Proceedings of Science, PoS(NIC-IX)095

Freedman, W. L., Madore, B. F., Gibson, B. K. 2001, ApJ, 553, 47

Fryxell, B. A., Arnett, W. D. 1981, ApJ, 243, 994

Fuhrmann, K. 1998, A&A, 338, 161

Fuhrmann, K. 2008, MNRAS, 384, 173

Garnett, D. R. 1999, in: Y.-H. Chu, N. Suntzeff, J. Hesser, D. Bohlender (eds.), *New Views of the Magellanic Clouds* (ASP, San Francisco), 266

Garnett, D. R. 2004, in: C. Esteban, R. J. García López, A. Herrero, F. Sánchez (eds.), *Cosmochemistry* (Cambridge University Press, Cambridge), 171

Geier, S., Nesslinger, S., Heber, U., **Przybilla, N.**, Napiwotzki, R., Kudritzki, R. P. 2007, A&A, 464, 299

Ghez, A. M., Salim, S., Hornstein, S. D., et al. 2005, ApJ, 620, 744

Giddings, J. R. 1981, Ph. D. Thesis, Univ. London

Gieren, W., Pietrzyński, G. Bresolin, F., et al. 2005, ESO Messenger, 121, 23

Gies, D. R., Lambert, D. L. 1992, ApJ, 387, 673

Gnedin, O. Y., Gould, A., Miralda-Escudé, J., Zentner, A. R. 2005, ApJ, 634, 344

Gratton, R. G., Carretta, E., Claudi, R., Lucatello, S., Barbieri, M. 2003, A&A, 404, 187

Grevesse, N., Sauval, A. J. 1998, Space Sci. Rev., 85, 161

Grevesse, N., Asplund, M., Sauval, A. J. 2007, Space Sci. Rev., 130, 105

Groth, H. G. 1961, ZAp, 51, 231

Gualandris, A., Portegies Zwart, S. 2007, MNRAS, 376, L29

Gummersbach, C. A., Kaufer, A., Schaefer, D. R., et al. 1998, A&A, 338, 881

Heber, U., Edelmann, H., Napiwotzki, R., Altmann, M., Scholz, R.-D. 2008, A&A, 483, L21

Heger, A., Langer, N. 2000, ApJ, 544, 1016

Heger, A., Fryer, C. L., Woosley, S. E., Langer, N., Hartmann, D. H. 2003, ApJ, 591, 288

Heger, A., Woosley, S. E., Spruit, H. C. 2005, ApJ, 626, 350

Hillier, D. J., Miller, D. L. 1998, ApJ, 496, 407

Hills, J. G. 1988, Nature, 331, 687

Hirsch, H. A., Heber, U., O'Toole, S. J., Bresolin, F. 2005, A&A, 444, L61

Honda, S., Aoki, W., Kajino, T., et al. 2004, ApJ, 607, 474

Hou, J. J., Prantzos, N., Boissier, S. 2000, A&A, 362, 921

Hummer, D. G., Berrington, K. A., Eissner, W., et al. 1993, A&A, 279, 298

Hunter, I., Dufton, P. L., Smartt, S. J., et al. 2007, A&A, 466, 277

Israelian, G., Rebolo, R., Basri, G., Casares, J., Martín, E. L. 1999, Nature, 401, 142

Jensen, A. G., Rachford, B. L., Snow, T. P. 2007, ApJ, 654, 955

Johansson, S. 2005, in: H. U. Käufl, R. Siebenmorgen, A. Moorwood (eds.), *High Resolution Infrared Spectroscopy in Astronomy* (Springer Verlag, Berlin), 62

Käufl, H.U., Ballester, P., Biereichel, P., et al. 2004, Proc. SPIE, 5492, 1218

Kaufer, A., Stahl, O., Tubbesing, S., et al. 1999, ESO Messenger, 95, 8

Kennicutt, R. C., Jr., Bresolin, F., Garnett, D. R. 2003, ApJ, 591, 801

Kilian, J. 1992, A&A, 262, 171

Kilian, J. 1994, A&A, 282, 867

Kippenhahn, R., Weigert, A. 1990, *Stellar Structure and Evolution* (Springer Verlag, Berlin)

Kobayashi, C., Umeda, H., Nomoto, K., Tominaga, N., Ohkubo, T. 2006, ApJ, 653, 1145

Korn, A. J., Keller, S. C., Kaufer, A., et al. (**Przybilla, N.**) 2002, A&A, 385, 143

Korn, A. J., Nieva, M. F., Daflon, S., Cunha, K. 2005, ApJ, 633, 899

Kudritzki, R. P. 1973, A&A, 28, 103

Kudritzki, R. P. 1998, in: A. Aparicio, A. Herrero, F. Sánchez (eds.), *Stellar Astrophysics for the Local Group* (Cambridge University Press, Cambridge), 149

Kudritzki, R. P., **Przybilla, N.** 2003, in: D. Alloin, W. Gieren (eds.), *Stellar Candles for the Extragalactic Distance Scale* (Springer Verlag, Berlin), 123

Kudritzki, R. P., Puls, J., Lennon, D. J., et al. 1999, A&A, 350, 970

Kudritzki, R. P., Bresolin, F., **Przybilla, N.** 2003, ApJ, 582, L83

Kudritzki, R. P., Urbaneja, M. A., Bresolin, F., **Przybilla, N.**, Gieren, W., Pietrzyński, G. 2008, ApJ, 681, 269

Kupka, F., Ryabchikova, T. A., Weiss, W. W., et al. 1996, A&A, 308, 886

Kurucz, R. L. 1993, Kurucz CD-ROM No. 13 (SAO, Cambridge, Mass.)

Lanz, T., Hubeny, I. 2003, ApJS, 146, 417

Lennon, D. J., Dufton, P. L. 1989, A&A, 225, 439

Lenorzer, A., Mokiem, M. R., de Koter, A., Puls, J. 2004, A&A, 422, 275

Leonard, P. J. T. 1991, AJ, 101, 562

Leone, F., Lanzafame, A. C., Pasquini, L. 1995, A&A, 293, 457

Lodders, K. 2003, ApJ, 591, 1220

Löckmann, U., Baumgardt, H., Kroupa, P. 2008, ApJ, 683, L151

López-Corredoira, M., Cabrera-Lavers, A., Mahoney, T. J., et al. 2007, AJ, 133, 154

López-García, Z., Adelman, S. J., Pintado, O. I. 2001, A&A, 367, 859

Lyubimkov, L. S., Rostopchin, S. I., Rachkovskaya, T., et al. 2005, MNRAS, 358, 193

Maeda, K., Nakamura, T., Nomoto, K., et al. 2002, ApJ, 565, 405

Maeda, K., Kawabata, K., Mazzali, P. A., et al. 2008, Science, 319, 1220

Maeder, A., Meynet, G. 2000, ARA&A, 38, 143

Maeder, A., Meynet, G. 2001, A&A, 373, 555

Maeder, A., Meynet, G. 2005, A&A, 440, 1041

Martins, F., Gillessen, S., Eisenhauer, F., et al. 2008, ApJ, 672, L119

Mashonkina, L., Korn, A. J., **Przybilla, N.** 2007, A&A, 461, 261

Matteucci, F. 2001, *The Chemical Evolution of the Galaxy* (Springer Verlag, Berlin)

Meyer, D. M., Cardelli, J. A., Sofia, U. J. 1997, ApJ, 490, L103

Meynet, G., Maeder, A. 2003, A&A, 404, 975

Mihalas, D. 1978, *Stellar Atmospheres*, 2nd edition (Freeman, San Francisco)

Morel, T., Butler, K. 2008, A&A, 487, 307

Nielsen, K., Wahlgren, G. M. 2000, A&A, 356, 146

Nieva, M. F. 2007, Ph. D. Thesis, Univ. Erlangen-Nuremberg & ON, Rio de Janeiro

Nieva, M. F., **Przybilla, N.** 2006, ApJ, 639, L39

Nieva, M. F., **Przybilla, N.** 2007, A&A, 467, 295

Nieva, M. F., **Przybilla, N.** 2008, A&A, 481, 199

Nomoto, K., Tominaga, N., Umeda, H., Kobayashi, C., Maeda, K. 2006, Nucl. Phys. A, 777, 424

Oey, M. S. 2003, in: K. van der Hucht, A. Herrero, C. Esteban (eds.), *A Massive Star Odyssey: From Main Sequence to Supernova* (ASP, San Francisco), 620

Pagel, B. E. J. 1997, *Nucleosynthesis and Chemical Evolution of Galaxies* (Cambridge University Press, Cambridge)

Pasquini, L., Avila, G., Allaert, E. 2000, Proc. SPIE, 4008, 129

Pfeiffer, M. J., Frank, C., Baumüller, D., Fuhrmann, K., Gehren, T. 1998, A&AS, 130, 381

Podsiadlowski, P., Nomoto, K., Maeda, K., et al. 2002, ApJ, 567, 491

Przybilla, N. 2002, Ph. D. Thesis, Univ. Munich

Przybilla, N. 2005, A&A, 443, 293

Przybilla, N., Butler, K. 2001, A&A, 379, 955

Przybilla, N., Butler, K. 2004a, ApJ, 609, 1181

Przybilla, N., Butler, K. 2004b, ApJ, 610, L61

Przybilla, N., Butler, K., Becker, S. R., Kudritzki, R. P., Venn, K. A. 2000, A&A, 359, 1085

Przybilla, N., Butler, K., Becker, S. R., Kudritzki, R. P. 2001a, A&A, 369, 1009

Przybilla, N., Butler, K., Kudritzki, R. P. 2001b, A&A, 379, 936

Przybilla, N., Butler, K., Heber, U., Jeffery, C. S. 2005, A&A, 443, L25

Przybilla, N., Butler, K., Becker, S. R., Kudritzki, R. P. 2006a, A&A, 445, 1099

Przybilla, N., Nieva, M. F., Edelmann, H. 2006b, Baltic Astronomy, 15, 107

Przybilla, N., Nieva, M. F., Heber, U., Jeffery, C. S. 2006c, Baltic Astronomy, 15, 163

Przybilla, N., Butler, K., Kudritzki, R. P. 2008a, in: G. Israelian, G. Meynet (eds.), *The Metal Rich Universe* (Cambridge University Press, Cambridge), 335

Przybilla, N., Nieva, M. F., Heber, U., et al. 2008b, A&A, 480, L37

Przybilla, N., Nieva, M. F., Tillich, A., et al. 2008c, A&A, 488, L51

Przybilla, N., Nieva, M. F., Heber, U., Butler, K. 2008d, ApJ, 684, L103

Przybilla, N., Nieva, M. F., Butler, K. 2008e, ApJ, submitted (`arXiv:0809.2403 [astro-ph]`)

Przybilla, N., Seifahrt, A., Butler, K., et al. 2008f, in: A. Moorwood (ed.), *Science with the VLT in the ELT era* (Springer Verlag, Berlin), in press

Przybylski, A. 1968, MNRAS, 139, 313

Przybylski, A. 1969, MNRAS, 146, 71

Przybylski, A. 1972, MNRAS, 159, 155

Puls, J., Kudritzki, R. P., Herrero, A., et al. 1996, A&A, 305, 171

Puls, J., Urbaneja, M. A., Venero, R., et al. 2005, A&A, 435, 669

Reid, M. J. 1993, ARA&A, 31, 345

Repolust, T., Puls, J., Hanson, M. M., et al. 2005, A&A, 440, 261

Roberts, W. W., Jr., Huntley, J. M., van Albada, G. D. 1979, ApJ, 233, 67

Rothman, L. S., Jacquemart, D., Barbe, A., et al. 2005, JQSRT, 96, 139

Roy, J.-R., Kunth, D. 1995, A&A, 294, 432

Rudolph, A. L., Fich, M., Bell, G. R., et al. 2006, ApJS, 162, 346

Rybicki, G. B., Hummer, D. G. 1991, A&A, 245, 171

Sandage, A., Tammann, G. A., Saha, A., et al. 2006, ApJ, 653, 843

Schiller, F., **Przybilla, N.** 2008, A&A, 479, 849

Schödel, R., Ott, T., Genzel, R., et al. 2002, Nature, 419, 694

Seaton, M. J., Yan, Y., Mihalas, D., Pradhan, A. K. 1994, MNRAS, 266, 805

Seifert, W., Appenzeller, I., Fuertig, W., et al. 2000, Proc. SPIE, 4008, 96

Sheinis, A. I., Bolte, M., Epps, H. W., et al. 2002, PASP, 114, 851

Smith, K. C. 1996, Ap&SS, 237, 77

Snow, T. P., Witt, A. N. 1996, ApJ, 468, L65

Sofia, U. J. 2004, in: A. N. Witt, G. C. Clayton, B. T. Draine (eds.), *Astrophysics of Dust* (ASP, San Francisco), 393

Sofia, U. J., Meyer, D. M. 2001, ApJ, 554, L221

Stasińska, G. 2005, A&A, 434, 507

Takeda, Y., Takada-Hidai, M. 1998, PASJ, 50, 629

Takeda, Y., Takada-Hidai, M. 2000, PASJ, 52, 113

Trundle, C., Dufton, P. L., Hunter, I., et al. 2007, A&A, 471, 625

Urbaneja, M. A., Herrero, A., Bresolin, F., et al. (**Przybilla, N.**) 2005, ApJ, 622, 862

Urbaneja, M. A., Kudritzki, R. P., Bresolin, F., **Przybilla, N.**, Gieren, W., Pietrzyński, G. 2008, ApJ, 684, 118

Van Regemorter, H. 1962, ApJ, 136, 906

Venn, K. A. 1995a, ApJS, 99, 659

Venn, K. A. 1995b, ApJ, 449, 839

Venn, K. A., **Przybilla, N.** 2003, in: C. Charbonnel, D. Schaerer, G. Meynet (eds.), *CNO in the Universe* (ASP, San Francisco), 20

Venn, K. A., McCarthy, J. K., Lennon, D. J., **Przybilla, N.**, Kudritzki, R. P., Lemke, M. 2000, ApJ, 541, 610

Venn, K. A., Lennon, D. J., Kaufer, A., McCarthy, J. K., **Przybilla, N.**, et al. 2001, ApJ, 547, 765

Venn, K. A., Kaufer, A., Tolstoy, E., et al. (**Przybilla, N.**) 2003, in: K. van der Hucht, A. Herrero, C. Esteban (eds.), *A Massive Star Odyssey: From Main Sequence to Supernova* (ASP, San Francisco), 30

Verdugo, E., Talavera, A., Gómez de Castro, A. I. 1999, A&A, 346, 819

Vogt, S. S., Allen, S. L., Bigelow, B. C., et al. 1994, Proc. SPIE, 2198, 362

Vrancken, M., Butler, K., Becker, S. R. 1996, A&A, 311, 661

Wolf, B. 1971, A&A, 10, 383

Wolf, B. 1972, A&A, 20, 275

Wolf, B. 1973, A&A, 28, 335

Yu, Q., Madau, P. 2007, MNRAS, 379, 1293

Yu, Q., Tremaine, S. 2003, ApJ, 599, 1129

Zaritsky, D., Kennicutt, R. C., Jr., Huchra, J. P. 1994, ApJ, 420, 87

Acknowledgements

It is my pleasure to thank Uli Heber, for paving the way for this venture, for encouragement, advice and support over the past years in Bamberg, and for lessons in diplomacy. I also want to thank Wolf-Rainer Hamann and Erhard Steffens for their willingness to accompany the progress of this work as mentors.

I am deeply grateful to many colleagues and friends for support, advice, discussions and collaboration – Keith Butler, Rolf Kudritzki, Joachim Puls, the Bamberg, Munich, Hawaii, and Tenerife crowds, and many, many more (you know who I mean). Special thanks to Fernanda Nieva, Markus Firnstein and Florian Schiller for getting enthusiastic about realising ideas.

Schließlich möchte ich meinen Eltern und meiner Partnerin für ihre Geduld und Unterstützung während der letzten Jahre danken.

Appended Papers

Model Development & Analysis Methodology

Appendix A: N. Przybilla & K. Butler, *Non-LTE Line Formation for Hydrogen Revisited*, Astrophysical Journal, 609, 1181–1191 (2004)

Appendix B: N. Przybilla, *Non-LTE Modelling of the He I 10830 Å Line in Early-Type Main Sequence Stars*, Astronomy & Astrophysics, 443, 293–296 (2005)

Appendix C: N. Przybilla, K. Butler, S. R. Becker & R. P. Kudritzki, *Quantitative Spectroscopy of BA-type Supergiants*, Astronomy & Astrophysics, 445, 1099–1126 (2006)

Appendix D: M. F. Nieva & N. Przybilla, C II *Abundances in Early-Type Stars: Solution to a Notorious Non-LTE Problem*, Astrophysical Journal, 639, L39–L42 (2006)

Appendix E: M. F. Nieva & N. Przybilla, *Hydrogen and Helium Line Formation in OB Dwarfs and Giants. A hybrid Non-LTE Approach*, Astronomy & Astrophysics, 467, 295–309 (2007)

Appendix F: F. Schiller & N. Przybilla, *Quantitative spectroscopy of Deneb*, Astronomy & Astrophysics, 479, 849–858 (2008)

Appendix G: M. F. Nieva & N. Przybilla, *Carbon Abundances of Early B-type Stars in the Solar Vicinity. Non-LTE Line-formation for C II/III/IV and Self-consistent Atmospheric Parameters*, Astronomy & Astrophysics, 481, 199–216 (2008)

Galactochemical Evolution

Appendix H: N. Przybilla, M. F. Nieva, & K. Butler, *A Cosmic Abundance Standard: Chemical Homogeneity of the Solar Neighbourhood & the ISM Dust-Phase Composition*, Astrophysical Journal Letters, submitted (`arXiv:0809.2403 [astro-ph]`)

Hypervelocity Stars

Appendix I: N. Przybilla, M. F. Nieva, U. Heber, M. Firnstein, K. Butler, R. Napiwotzki & H. Edelmann, *LMC Origin of the Hyper-velocity Star HE 0437–5439. Beyond the Supermassive Black Hole Paradigm*, Astronomy & Astrophysics, 480, L37–L40 (2008)

Appendix J: N. Przybilla, M. F. Nieva, A. Tillich, U. Heber, K. Butler & W. R. Brown, *HVS 7: A Chemically Peculiar Hyper-velocity Star*, Astronomy & Astrophysics, 488, L51–L54 (2008)

Appendix K: N. Przybilla, M. F. Nieva, U. Heber & K. Butler, *HD 271791: An Extreme Supernova Run-away B Star Escaping from the Galaxy*, Astrophysical Journal, 684, L103–L106 (2008)

Extragalactic Stellar Astronomy

Appendix L: R. P. Kudritzki, F. Bresolin & N. Przybilla, *A New Extragalactic Distance Determination Method Using the Flux-weighted Gravity of Late B and Early A Supergiants*, Astrophysical Journal, 582, L83–L86 (2003)

Appendix M: R. P. Kudritzki, M. A. Urbaneja, F. Bresolin, N. Przybilla, W. Gieren & G. Pietrzyński, *Quantitative Spectroscopy of 24 A Supergiants in the Sculptor Galaxy NGC 300: Flux-weighted Gravity-Luminosity Relationship, Metallicity, and Metallicity Gradient*, Astrophysical Journal, 681, 269–289 (2008)